AD-A105 235 UNITED TECHNOLOGIES RESEARCH CENTER EAST HARTFORD CT F/G 7/4
INVESTIGATION OF THE CARS SPECTRUM OF WATER VAPOR.(U)
AUG 81 J A SHIRLEY, R J HALL F33615-80-C-2061
UNCLASSIFIED UTRC/R81-955278-10 AFWAL-TR-81-2075 NL

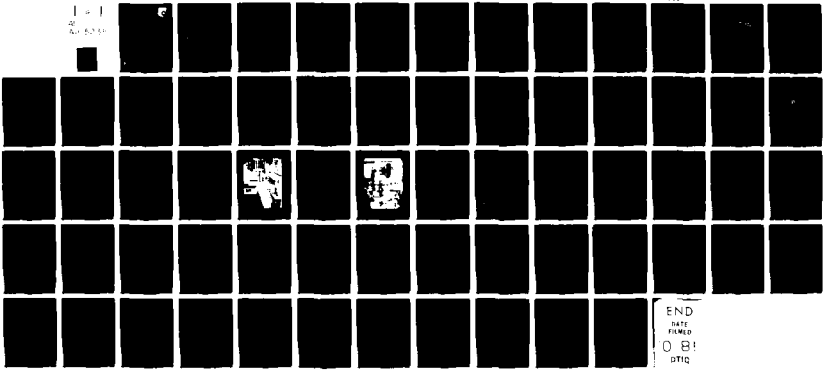

END
DATE FILMED
08
DTIC

AFWAL-TR-81-2075

INVESTIGATION OF THE CARS SPECTRUM OF WATER VAPOR

J.A. Shirley and R.J. Hall

United Technologies Research Center
East Hartford, Connecticut 06108

Final Report for Period: July 1980 — March 1981

AUGUST 1981

AERO PROPULSION LABORATORY
AIR FORCE WRIGHT AERONAUTICAL LABORATORIES
AIR FORCE SYSTEMS COMMAND
WRIGHT-PATTERSON AIR FORCE BASE, OHIO 45433

NOTICE

When Government drawings, specifications, or other data are used for any purpose other than in connection with a definitely related Government procurement operation, the United States Government thereby incurs no responsibility nor any obligation whatsoever; and the fact that the government may have formulated, furnished, or in any way supplied the said drawings, specifications, or other data, is not to be regarded by implication or otherwise as in any manner licensing the holder or any other person or corporation, or conveying any rights or permission to manufacture use, or sell any patented invention that may in any way be related thereto.

This report has been reviewed by the Office of Public Affairs (ASD/PA) and is releasable to the National Technical Information Service (NTIS). At NTIS, it will be available to the general public, including foreign nations.

This technical report has been reviewed and is approved for publication.

PROJECT ENGINEER

ROBERT R. BARTHELEMY
Chief, Energy Conversion Branch
Aerospace Power Division

FOR THE COMMANDER

JAMES D. REAMS
Chief, Aerospace Power Division
Aero Propulsion Laboratory

"If your address has changed, if you wish to be removed from our mailing list, or if the addressee is no longer employed by your organization please notify POOC-3, W-PAFB, OH 45433 to help us maintain a current mailing list".

Copies of this report should not be returned unless return is required by security considerations, contractual obligations, or notice on a specific document.

Unclassified

SECURITY CLASSIFICATION OF THIS PAGE (When Data Entered)

REPORT DOCUMENTATION PAGE

READ INSTRUCTIONS BEFORE COMPLETING FORM

1. REPORT NUMBER: AFWAL-TR-81-2075	2. GOVT ACCESSION NO.: AD-A105235
3. RECIPIENT'S CATALOG NUMBER	
4. TITLE (and Subtitle): INVESTIGATION OF THE CARS SPECTRUM OF WATER VAPOR	5. PERIOD COVERED: Final Report, July 1980 - May 1981
6. PERFORMING ORG. REPORT NUMBER: UTRC R81-955278-10	
7. AUTHOR(s): J. A. Shirley and R. J. Hall	8. CONTRACT OR GRANT NUMBER(s): F33615-80-C-2061
9. PERFORMING ORGANIZATION NAME AND ADDRESS: United Technologies Corporation, Research Center, 400 Main Street, East Hartford, Ct. 06108	10. PROGRAM ELEMENT, PROJECT, TASK AREA & WORK UNIT NUMBERS: 2301-S1-20
11. CONTROLLING OFFICE NAME AND ADDRESS: Aerospace Propulsion Laboratory (AFWAL/POOC-3), Air Force Wright Aeronautical Laboratories	12. REPORT DATE: August 1981 13. NUMBER OF PAGES: 60
14. MONITORING AGENCY NAME & ADDRESS (if different from Controlling Office)	15. SECURITY CLASS. (of this report): Unclassified 15a. DECLASSIFICATION DOWNGRADING SCHEDULE

16. DISTRIBUTION STATEMENT (of this Report)

Approval for public release; distribution unlimited

17. DISTRIBUTION STATEMENT (of the abstract entered in Block 20, if different from Report)

18. SUPPLEMENTARY NOTES

19. KEY WORDS (Continue on reverse side if necessary and identify by block number)

H_2O CARS
Coherent anti-Stokes Raman spectroscopy
Water vapor
Raman

20. ABSTRACT (Continue on reverse side if necessary and identify by block number)

The coherent anti-Stokes Raman spectrum of water vapor was measured and compared with CARS code calculations to facilitate diagnostics of this important combustion product. Measurements were made with mixtures of H_2O and a diluent gas heated to 450-800 K in a test cell at atmospheric pressure. The experimental spectra were computer fit to calculations to deduce H_2O Raman linewidths. The self broadening coefficient was found to be

DD FORM 1 JAN 73 1473 EDITION OF 1 NOV 65 IS OBSOLETE
S N 0102-LF-014-6601

Unclassified 409252
SECURITY CLASSIFICATION OF THIS PAGE (When Data Entered)

0.5 cm^{-1}/atm at 773°K and to depend inversely on the temperature. N_2 and CO_2 broadening coefficients are comparable, essentially independent of temperature at 0.17 cm^{-1}/atm over this range. Measurements were also made in the post-reaction region of stoichiometric CH_4-air flames at 1670 and 2070°K. The linewidth was inferred to be 0.24-0.25 cm^{-1}/atm in both flames.

Investigation of the CARS Spectrum of Water Vapor

TABLE OF CONTENTS

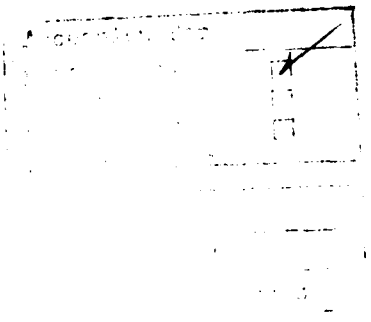

A

SUMMARY

The specific objective of this investigation was to verify and refine a theoretical computer code developed at the United Technologies Research Center which calculates the coherent anti-Stokes Raman spectrum of water vapor. The more general motivation for this work was to develop CARS as a diagnostic tool to measure water vapor temperature and concentration in combustion systems.

To verify the CARS code, the spectrum of H_2O was measured in premixed methane-air flames and in a temperature-controlled, heated cell operated at atmospheric pressure with varying compositions of water vapor and a diluent gas. The temperature measured by thermocouples ranged from approximately 400-800 K in the heated cell, to 1700-2100 K in the flames. The H_2O concentration in the heated cell was determined from saturation conditions, established in a separately-heated vessel through which the mixture flowed prior to entering the heated cell. The concentration was varied from approximately 3.5 to 100 percent, for N_2, CO_2 and Ar collision partners. By least-squares fitting the experimental spectra to calculations for different Raman linewidths, the broadening coefficients for H_2O, N_2 and CO_2 have been inferred. The self-broadened linewidth was found to obey an inverse dependence on temperature at the lower temperatures with the dependence weakening and becoming essentially constant as flame temperatures were reached. Self-broadening was found to be about 2.5 times more effective at the higher cell temperatures than broadening by N_2 or CO_2, which were comparable. The inferred broadening parameters are in general agreement with microwave measurements of pure rotational transitions.

It is concluded that the UTRC H_2O CARS code satisfactorily describes the H_2O spectrum near atmospheric pressure over the entire measured range of temperature and gas composition. It appears feasible to make concentration measurements from the shape of the CARS spectrum in premixed hydrocarbon-fueled flames. In hydrogen-air flames it will be necessary to measure H_2O concentrations from integrated intensities where the concentration is greater than 20 percent. In situ referencing techniques will be valuable for these measurements. The Raman linewidth, though, appears to be known well enough for these measurements.

INTRODUCTION

Water vapor is a major product of air-fed hydrogen- and hydrocarbon-fueled combustion. Its concentration in combustion products can be used to determine the extent of chemical reaction and overall combustion efficiency. Therefore, measurements of the temperature and, in particular, the concentration of this species in real combustion systems should contribute to a greater understanding of combustion, leading ultimately perhaps to better fuel efficiency and economy. For this reason accurate diagnostic measurements of this species appear important to future combustion improvements. Traditionally, various types of physical probes have been inserted into aerodynamic and combusting flows to measure flow properties. In combustion systems, however, these probes are confronted with conditions which often exceed material capabilities. In addition, the presence of a foreign object can perturb the flow, producing misleading and erroneous results.

Optical techniques are being developed to overcome these difficulties. The proliferation of high power lasers has enabled the application of many new or previously esoteric optical techniques to combustion research. Among these are laser Dopper velocimetry (LDV), laser-induced fluorescence (LIF), spontaneous Raman scattering, and coherent Raman techniques such as coherent anti-Stokes Raman spectroscopy (CARS). LDV can be used to map the combustion velocity field and, thus, is an important adjunct to the other techniques, which are used to measure temperature and concentration. At present, spontaneous Raman scattering and CARS appear better suited to major species measurements, while laser-induced fluorescence appears most suited to the measurement of species in trace concentrations, such as flame radicals.

For H_2O, which occurs usually in moderate concentrations in combustion, either spontaneous Raman scattering or CARS, then, are potentially useful non-intrusive diagnostic approaches. Spontaneous Raman scattering often is limited in combustion applications by laser-induced interferences because of its weak and incoherent signal. In contrast, CARS produces a strong, coherent beam that is frequency up-shifted and, therefore, overcomes these limitations. Because of this, the use of CARS is rapidly increasing and it is becoming the preferred approach for spatially resolved measurements of temperature and major species concentrations in practical combustion systems. Its feasibility for diagnostics has been demonstrated in such realistic environments as combustion tunnels (Ref. 1-3), and internal combustion engines (Refs. 4 and 5).

Recently there has been a considerable effort to understand the Raman spectroscopy of water vapor to facilitate combustion measurements. The Raman cross section was measured by Penney and Lapp at General Electric (Ref. 6). These same workers determined the effect of temperature on the spectrum at temperatures from 150 to 350 C. The favorable agreement of these measurements

with spectral contours computed by Bribes, Gaufres, and Monan at Montpellier in France was reported in a paper jointly authored with the GE workers in 1976 (Ref. 7). Later, agreement between flame measurements (Ref. 8) and calculations was reported by these same investigators (Ref. 9). In addition to these combustion related studies, there has been a number of Raman studies of liquid water to determine its structure and the effects of hydrogen bonding (Ref. 10). The investigation of the CARS spectrum of water has not been as extensive as spontaneous Raman. The CARS spectrum of liquid water was measured by Itzkan and Leonard (Ref. 11). The first CARS spectrum of water vapor in a flame was reported by Hall, Shirley and Eckbreth (Ref. 12). The agreement between the experimental spectrum and modeling calculation at the one temperature measured was very good. CARS spectra of H_2O at room temperature and ~500 K were reported by Roh et al, however few details were given (Ref. 13). Quite recently, Farrow et al at Sandia Labs obtained a single pulse spectrum of the water vapor in air using a technique which eliminates background interference (Ref. 14).

To develop CARS as reliable technique for combustion temperature and concentration measurements, it is necessary to develop a computer code to calculate spectra. Analyzing data requires the compilation of a library of simulated spectra for a range of species concentration and temperature to compare to experimental spectra. The calculation of CARS spectra is more complex than the calculation of Raman spectra. The nonlinear nature of the CARS process gives rise to interference effects between adjacent transitions of the molecule being studied and between these transitions and the background of all other species present. Water vapor, because it is a triatomic asymmetric top molecule, has a complicated spectrum, which is quite sensitive to assumed spectroscopic constants and parameters, such as energy levels, statistical weights, linewidths, etc. The objective of this investigation was to measure CARS spectra of H_2O, over a wide variety of known conditions relevant to combustion, and to use these measurements to verify and, if necessary, modify the existing UTRC CARS computer code. To put these studies in better focus it should be kept in mind that H_2O is largely a product in combustion, and as such would not be an ideal thermometric species, although the spectrum is expected to be quite sensitive to temperature (Ref. 12). The effect of temperature on the spectrum must be understood though to determine H_2O concentrations from CARS spectra.

As part of this contract, the UTRC H_2O CARS computer code was delivered to the Aeronautical Systems Divisions (WPAFB) and NASA Langley Research Center. The operation of the code was demonstrated at both facilities and user's manuals for the code were delivered.

In the next section of this report, CARS theory is briefly described. This is followed by a section detailing the vibrational Raman spectroscopy of H_2O, and how the CARS spectrum is calculated. Predicted CARS spectra of H_2O and the sensitivity to temperature, concentration, and assumed Raman linewidth are also described in this section. The experimental apparatus, and the results of measurements in a heated cell and flames are described next. Following this, the experimental spectra are compared in detail to the calculated spectra. The experimental data are fit to calculated spectra for various temperatures, water vapor concentrations and collision partners to infer the dependence of linewidth on mixture composition and temperature. Finally, the investigations are summarized and, conclusions and recommendations are made with respect to how CARS can be used for diagnostic measurements of H_2O.

COHERENT ANTI-STOKES RAMAN SPECTROSCOPY

This section opens with a brief review of the principles of coherent anti-Stokes Raman spectroscopy. The fundamental expression describing the response of H_2O and the surrounding species to impressed laser fields is presented, and methods for extracting temperature and species concentration from CARS spectra are discussed. Next, the relevant spectroscopy of H_2O is described. The energy level structure, Raman selection rules, Raman linewidths and non-resonant susceptibility are discussed. The section concludes by presenting calculations of H_2O CARS spectra and studies of sensitivity to temperature, linewidth and concentration.

CARS Theory and Measurements

The theory and application of CARS are well explained in several reviews which have appeared recently (Refs. 15-18). The basic process is shown schematically in Fig. 1. Two incident laser beams at frequencies ω_1 and ω_2 (termed the pump and Stokes respectively) wave mix through a nonlinear interaction to generate various frequency combinations including a frequency at $\omega_1 + (\omega_1 - \omega_2) \equiv \omega_3$. When the difference frequency, $\omega_1 - \omega_2$, is resonant with a Raman-allowed transition (see Fig. 1) of a specie in the interaction region, the conversion to the third frequency can be quite strong. In most experiments, vibrational resonances of molecules are probed. Since a molecular vibration can have many rotational sub-levels excited, a species typically has several resonances which are sensitive to temperature. Therefore, temperature and, it can also be shown, concentration information is contained in the CARS spectrum. The spectrum is generated in either of two ways, also illustrated in Fig. 1. In the first method, the Stokes frequency is swept relative to the fixed pump frequency, so that the entire molecular CARS spectrum is generated sequentially. This technique is precluded from use for diagnostics of unsteady situations because of the nonlinear dependence of CARS on temperature and density. The second method overcomes this limitation by using a broadband Stokes laser (Ref. 19) to generate the entire CARS spectrum simultaneously. This method was used for the measurements reported here.

The optical beams in Fig. 1 are represented as crossing at an angle to each other; in fact, because CARS is a coherent process a relationship between the propagation vectors of the fields must be satisfied for efficient signal generation to occur. In gases, which are essentially dispersionless, this relationship (called phase matching) is satisfied when the beams are aligned collinear with each other. In many diagnostic circumstances, collinear phase matching leads to poor and ambiguous spatial resolution. This difficulty is circumvented by employing crossed-beam phase matching, such as BOXCARS (Ref. 20), or a variation thereof (Refs. 5 and 21). In these approaches the pump and

- APPROACH

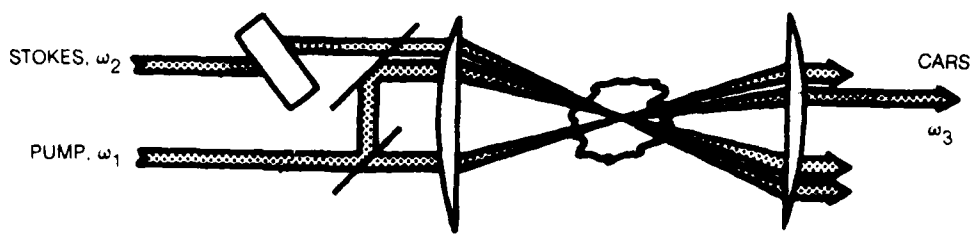

- ENERGY LEVEL DIAGRAM

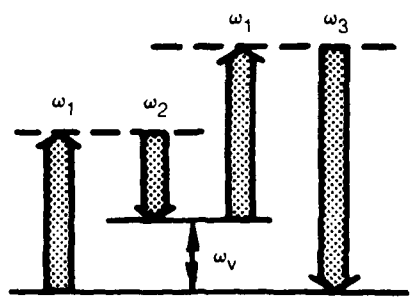

- SPECTRUM

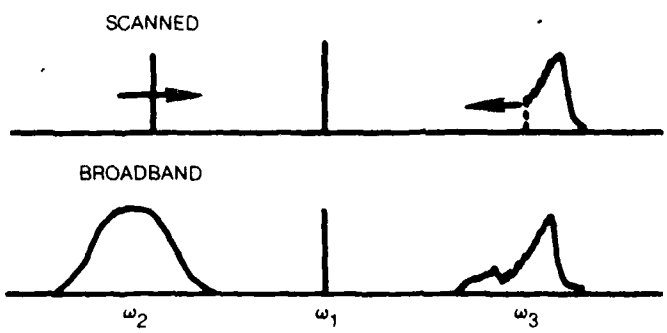

Figure 1. Coherent Anti-Stokes Raman Spectroscopy (CARS)

Stokes beams are crossed, in accordance with the phase matching relationship. Generation occurs where the beams intersect, and very high spatial resolution is possible with focussed beams. The intersecting laser beams need not be coplanar (Ref. 22 and 23) and experimental simplifications can be gained using three-dimensional phase matching.

The CARS signal is proportional to the square of the modulus of the third-order electric susceptibility, $\chi^{(3)}_{ijkl}(-\omega_3, \omega_1, \omega_1, -\omega_2)$ (Ref. 15), which is a fourth rank tensor. The subscripts correspond to the polarization directions of the four fields in the order listed in the parentheses. For vibrational Q-branch transitions, i.e. $\Delta J=0$, involving a depolarized mode, the susceptibility in the isolated line approximation can be written for detuning frequency, $\Delta\omega_j \equiv \omega_1 - \omega_2 - \omega_j$, small with respect to the Raman frequency ω_j as

$$\chi^{(3)} = \frac{2c^4}{\hbar\omega_2^4} N \sum_j \frac{\Delta_j (\partial\sigma/\partial\Omega_j)}{2\Delta\omega_j - i\Gamma_j} + \chi^{nr} \qquad (1)$$

where the summation over j includes all Q-branch transitions. In this equation N is the number density of the Raman active species, $(\partial\sigma/\partial\Omega)j$ is the Raman cross section, Γ_j is the Raman linewidth, and Δ_j is the fractional population difference between the levels involved in the transition. χ^{nr} is the nonresonant susceptibility which arises from the orbital electrons of all species present and from remote Raman resonances.

CARS spectra are more complicated than spontaneous Raman spectra because the signal depends on $|\chi^{(3)}|^2$. Constructive and destructive interferences can arise between neighboring transitions depending on the separation between the transitions and degree of overlap determined by the Raman linewidth. Interference can also result from the nonresonant susceptibility. For most molecules of interest to combustion, it has been found that these effects can be handled numerically by CARS computer codes. These codes need to be validated, however, because they require a knowledge of energy levels, transition strengths and linewidths which are not all as well know, a priori, as required.

Once one has a validated code, reliable temperature information can be obtained by comparing a measured spectrum to calculated spectra. This is also true for concentration measurements, but other considerations arise.

When the polarizations of all the fields are aligned in one direction, the detectability of a Raman active species in a mixture is limited by the

background nonresonant susceptibility. For a single resonance the resonant part of $\chi^{(3)}$ can be expanded into a real and an imaginary part, so that the square of the absolute value is

$$|\chi^{(3)}|^2 = |\chi' + i\chi'' + \chi^{nr}|^2 \qquad (2)$$

$$= \chi'^2 + 2\chi'\chi^{nr} + \chi^{nr^2} + \chi''^2 .$$

χ' and χ'', the real and imaginary parts of the resonant susceptibility, have a functional form depending on the detuning frequency, $\Delta\omega_j$, similar to the real and imaginary parts of the refractive index in the neighborhood of an absorption line. The real part has a dispersive lineshape and the imaginary part has a resonance shape. For a species in high concentration, $\chi^2 \approx \chi'^2 + \chi''^2$ which is just a resonant lineshape. However, for a species in low concentration, $\chi^2 \approx 2\chi'\chi^{nr} + \chi^{nr2}$, which implies an essentially constant background modulated by a dispersive term proportional to the measured species concentration. When this concentration is very low, the molecular signature disappears into the constant background. This has been perceived as a limitation to CARS because it means that a minor species can only be measured down to a certain level, typically of the order of 0.5 percent.

Several approaches to overcome this limitation in detectable concentration have been devised (Refs. 24-29). These techniques will not be discussed except to point out that differences in the polarization or temporal response properties between the resonant and nonresonant contributions can be exploited, in some cases, to eliminate the effect of the background nonresonant susceptibility. Eckbreth and Hall (Ref. 30) have shown that this cannot be done, however, without a loss in overall signal, at least for the polarization technique.

The presence of the background susceptibility should not be regarded as being detrimental, since some important advantages accrue from its existence. When the species of interest is in low concentration, a spectrum displaying modulation is produced. The amount of the modulation depends on the molecular species, its relative concentration and the background susceptibilty. These effects can be modeled by computer codes assuming a value for the background susceptibility. To the extent that the background susceptibility is known, the concentration can be determined from the CARS spectral shape (Ref. 31) which is considerably simpler in terms of the amount of equipment required than determinations from absolute intensities. This method of concentration measurement is examined for H_2O is this report.

When the molecular species is abundant, there is no longer any appreciable modulation. In this case concentration must be obtained from absolute intensities. The response of the CARS signal (spectrally integrated) to different concentrations of the molecular species must be determined and a reference cell to compensate for pulse-to-pulse laser power fluctuations, account for small misalignment, and serve as a calibration standard must be used. When the medium being probed is turbulent or contains droplets or particles then reference cells may not be appropriate because of beam steering, defocussing or attenuation. In these situations the background nonresonant susceptibility can be used as an in situ reference. Realizations of this concept which involve a second Stokes reference laser (Ref. 32) or polarization orientation (Refs. 14 and 33) have been proposed and demonstrated and are receiving considerable attention.

H_2O Spectroscopy

H_2O is an example of an asymmetric top molecule in which the three principal moments of inertia are all different. It possesses three fundamental vibrational modes; these are denoted by ν_1, ν_2, and ν_3, and correspond to symmetric stretching, bending, and asymmetric stretching motions, respectively. A vibrational quantum state is therefore denoted by $(\nu_1\nu_2\nu_3)$, where ν_i is the vibrational quantum number of the ith mode. Of the three fundamental modes, only the symmetric stretch mode, with a shift of 3657 cm^{-1} is Raman active (Ref. 6). At low temperatures only the H_2O ground state is significantly populated, and only Raman transitions belonging to the fundamental (000) → (100) band will be important. The first state in the bending mode has an energy of 1597 cm^{-1} however; because it can be significantly populated at flame temperatures, a vibrational "hot" band corresponding to (010) → (110) transitions can become important as well.

In diatomic molecules, the rotational substructure is characterized principally by a quantum number J which gives the total rotational angular momentum as $\hbar J(J+1)$. Each rotational quantum state in turn has a degeneracy equal to 2J+1, corresponding to the possible values of the magnetic, or azimuthal quantum number $m(-J \leq m \leq J)$. The component of rotational angular momentum measured along an arbitrary axis in space will be given by $m\hbar$. Similarly, a symmetric top molecule is characterized by the three rotational quantum numbers J, K, and m, where the additional quantum number K gives the component of angular momentum along the axis of symmetry; K takes on the values $-J \leq K \leq J$, and the rotational energy levels are given by the explicit formula

$$E(J,K) = BJ(J+1) + (A-B)K^2 \qquad (3)$$

As is discussed by Herzberg, (Ref. 34) in passing from the symmetric to the asymmetric top, there is no longer an explicit formula which can be written for the energy levels, and there are in general 2J+1 different levels for each value of J. Because a quantum number having a physically identifiable meaning cannot be assigned to these different states, it is common practice to denote them by a pseudo quantum number τ having values in the range

$$-J \leq \tau \leq J \qquad (4)$$

The rotational energies for a particular value of J will generally increase as τ increases from -J to +J.

Because H_2O has two identical nuclei with nonzero spin, the symmetric and antisymmetric rotational levels have different statistical weights due to nuclear spin statistics. The symmetry of the rotational level depends on the value of τ; thus, for the vibrational levels of interest, states in which τ is odd have three times the nuclear spin statistical weight of states in which τ is even. Each J_τ states also possesses the usual 2J+1 magnetic or azimuthal degeneracy (m quantum number).

Water Molecule Energy Level Data

CARS calculations generally place very stringent requirements on energy-level accuracy because of the strong spectral interference effects which arise from the dependence of CARS intensity on the squared modulus of the third order nonlinear susceptibility. Fortunately, extensive tabulations of H_2O vibration-rotation energy levels based on absorption band measurements have been published by Camy-Peyret, Flaud, and Maillard (Refs. 35-37). A 977 line tabulation of their earlier, unpublished data has been compiled by R. Gaufres of Montpellier which contains energy level and wavelength data for transitions belonging to the fundamental band and such hot bands as (010) → (110), (100 → (200) and (020) → (120). This data set was used in theoretical calculations which gave good agreement with spontaneous Raman spectra of H_2O over the temperature range 293 to 1500 K (Ref. 9). A separate compilation by Hall of UTRC of published data was used in a theoretical calculation which gave good agreement with the first experimental H_2O flame CARS spectrum (Ref. 12). This compilation contained data for 633 lines belonging mainly to the fundamental, but also contained (010) → (110) hot band transitions. The Gaufres energy level tabulation was used by R. L. St. Peters of General Electric in theoretical calculations (Ref. 38) which also showed good agreement with the early UTRC flame spectrum. For the transitions of most interest, there are slight differences between the Hall and Gaufres compilations with slight resulting differences in calculated spectra. The Gaufres compilation was obtained by UTRC in an exchange

of data sets with G.E.; in the early stages of this contract, the results of using the two different energy level compilations were compared, and it was found that slightly better agreement was obtained by using the Gaufres data set. Thus, all data reduction was carried out with this data set, and it is included in the computer code to be delivered under the contract. As a result of the UTRC-GE data set exchange, R. L. St. Peters produced a combined data set containing 831 lines. Use of this energy level compilation in the UTRC CARS code produced only very minor changes in predicted spectra, however.

Raman Selection Rules for H_2O

The Raman selection rules for asymmetric rotors are discussed by Herzberg (Ref. 34). In general five branches corresponding to the selection rules $\Delta J = 0, \pm 1, \pm 2$ are expected, and, as Bribes, et. al., (Ref. 7) point out, approximately $1/4\ (2J+1)^2$ transitions would be expected for each value of J. The situation is greatly simplified, however, by the relatively small depolarization ($\rho < .06$) of the ν_1 mode (Ref. 6) which makes it possible to restrict attention to trace scattering (Q-branch transitions) obeying the greatly simplified selection rules $\Delta J = \Delta\tau = 0$. Thus, it is necessary to consider in the calculations only one Q-branch transition for each vibration-rotation state having significant population.

Raman Linewidths

Unlike spontaneous Raman spectra, which are simply an incoherent addition of contributions for neighboring transitions, CARS spectra do display sensitivity to the values of the pressure-broadened linewidths Γ_j (See Eq. 1). Whereas the spontaneous Raman intensity is roughly proportional to

$$I_{sp} \sim \sum_j \chi_j'' \tag{5}$$

the CARS intensity is proportional to

$$I_{CARS} \sim |\chi^{(3)}|^2 \sim \left(\sum_j \chi_j'\right)^2 + \left(\sum_j \chi_j''\right)^2 \tag{6}$$

and constructive and destructive interference effects will arise in CARS if the linewidths are of sufficient magnitude to cause overlap of adjacent transitions. As will be seen, a moderate sensitivity of predicted spectra to Raman linewidth is generally found. Greater knowledge of these widths will be important if H_2O CARS is to be a reliable diagnostic tool.

In a quantum mechanical sense, the pressure-broadened Raman linewidth represents the rate at which molecular collisions perturb the coherent molecular oscillation driven by the fields at ω_1 and ω_2. For Q-branch transitions in diatomic molecules, the linewidth is equivalent to the inelastic (rotational + vibrational) collision frequency if vibrational dephasing collisions are slow. It is expected that this will be the case for H_2O Q-branches as well; that is, only collisions which are inelastic as far as the radiating molecule is concerned contribute to the linewidth, and the linewidth is a measure of the collisional lifetimes of the states involved in the transition.

At the present time considerable Raman linewidth data are available for many molecules (see Ref. 39), but none for H_2O. An intuitive notion about these widths is that, because H_2O possesses such a large electric dipole moment (μ = 1.87 Debye), rotationally-inelastic collisions in H_2O would be highly efficient and, thus, lead to relatively large linewidths. Also, because rotational energy transfer is most efficient for near-resonant energy transfer, one would expect the linewidths to roughly decrease in magnitude with increasing J, and that foreign gas broadening would be less efficient than self-broadening, expectations consistent with results found in other molecules. The Doppler linewidth for forward scattering will generally be appreciably smaller than the inferred Raman linewidths, even at flame temperatures, and this effect can be ignored.

Indirect evidence that these expectations are valid is provided by limited experimental data and computer calculations for microwave (pure rotational dipole) transitions (Refs. 40 and 41). Microwave linewidths for self-broadening are as large as 1 cm^{-1} atm^{-1} and for N_2 and O_2 collision partners are $\sim$ 0.2 cm^{-1} atm^{-1} (Refs. 40 and 41). The computer calculations, based on the Anderson theory (Ref. 42), also show that the linewidths do in general decrease with increasing J, and that for a given J they decrease with increasing τ. It is difficult to make a formal connection between microwave (pure rotational) and Raman linewidths. While both are affected by rotationally inelastic collisions, the microwave widths can have contributions from collisions which change the rotational orientation or phase (Ref. 43). Vibration-rotation Raman linewidths, on the other hand, can have extra contributions from vibrationally inelastic and dephasing collisions.

Thus, nothing was directly known about H_2O Q-branch Raman linewidths at the time the contract was initiated. While theoretical calculations based on the Anderson theory or some of its improved versions (Refs. 44 and 45) could probably give reasonably accurate values for these quantities, such calculations were beyond the scope of this investigation. Thus, a semiempirical approach was taken in which computer calculations were fitted to test cell and flame data over a wide range of temperatures and mixture compositions using the Raman linewidth as a fitting parameter. As will be seen, good fits to the experimental

data were achieved for all of the data taken, and the resulting inferred linewidths are not inconsistent in magnitude with the microwave linewidth results of Refs. 40 and 41.

Background Susceptibility

It has been shown that the third-order electric susceptibility which governs the CARS intensity consists of a resonant contribution due to Raman active vibration-rotation transitions and a background contribution that is mainly of electronic origin. The essentially dispersionless background susceptibility interferes with the real part of the resonant contribution, and constitutes a baseline into which the desired resonant signal will disappear if the H_2O mole fraction is too small. As long as this lower detectivity limit is avoided, the interference with the background contribution gives rise to a characteristic modulation of the CARS spectrum which affords an opportunity to perform concentration measurements from spectral shapes, a unique feature of CARS. For relatively low concentrations of the Raman-active species, it can be easily shown that the CARS signature takes on the dispersive profile of the real resonant contribution:

$$\left|\chi^{(3)}\right|^2 \simeq \chi_{NR}^2 \left[1 + \frac{2N}{\chi_{NR}} \bar{\chi}'_R (\Delta\omega)\right] \tag{7}$$

where N is the H_2O number density and $\bar{\chi}'_R(\Delta\omega)$ is the per molecule contribution to the real part of the resonant susceptibility. Thus, in computer fitting to an experimental spectrum, there will be a family of solutions determined by N/χ_{NR} = constant that have the same dispersive profile. The inferred H_2O number density will, therefore, be subject to an uncertainty determined by the uncertainty in χ_{NR}, and it is important to know the background susceptibilities due to constituents such as N_2, CO_2, and H_2O itself. It is desirable to know these values not only for accurate species concentration measurements, but also for accurate thermometry using H_2O, because the background interference will affect the H_2O CARS signature even at the ~20% concentration levels expected in hydrocarbon-fueled flames. Rado (Ref. 46) and DeMartini, et al (Ref. 47) have reported values of χ_{NR} for many gases of interest, with the exception of H_2O. However, these reported values were normalized to an assumed value of $\chi^{(3)}$ for the Q(1) line of H_2 on resonance. Eckbreth and Hall (Ref. 30) found that use of a calculated value of $\chi^{(3)}$ for H_2 would lead to a scaling up of the Rado-DeMartini values by a factor of about 2.5, and that use of these revised values gave very good agreement with measurements of minority species CO CARS spectra. These revised values were therefore used in the calculations performed under this contract, and are summarized in Table 1.

TABLE 1

REVISED BACKGROUND SUSCEPTIBILITY VALUES*
(From Ref. 30)

Gas	$\chi^{nr}(x10^{18}cm^3/erg)$
He	2.78
Ar	11.63
D_2	9.75
N_2	10.13
O_2	9.75
NO	31.5
CH_4	22.13
C_2H_6	46.5
CO_2	15.0

*To be used in the following expression for $\chi^{(3)}$

$$\chi^{(3)} = \frac{2c^4}{\hbar\omega_2^4} N \sum_j \frac{\Delta_j (\partial\sigma/\partial\Omega)_j}{2\Delta\omega_j - i\Gamma_j} + \chi^{nr}$$

By comparing the relative strengths of nonresonant CARS signals from air with those from H_2/air and H_2-O_2 flames, Shirley, et al (Ref. 48) have deduced that the nonresonant susceptibility for H_2O is roughly a factor of two larger than that for N_2. There is some confirmation of this result in the work on Ward and Miller (Ref. 49) who found that the susceptibility governing field-induced second harmonic generation (FISHG), which also derives from $\chi^{(3)}$, is approximately a factor of two greater in the case of H_2O than in the case of N_2. Thus, in the calculations performed for this contract, χ_{NR} for H_2O is assumed to be two times the N_2 value given in Table 1. Because H_2O is often a minority species for many conditions of interest, and

because its spectrum is not very sensitive to the background when it is a majority species, none of the results to be presented is strongly sensitive to this assumption. For gas mixtures, the background susceptibility is computed by weighting in accordance with the mole fraction, and it is commonly assumed that the susceptibility varies as 1/T at constant pressure.

Predicted H_2O Spectra

The calculation of the third order electric susceptibility governing the H_2O CARS spectrum is a straightforward procedure. Referring to Eq. (1), it is only necessary to calculate a Boltzmann population difference factor for each Q-branch transition, to compute a sum of complex Lorentzian resonant contributions, add in the background contribution, and take the squared modulus. The normalized Boltzmann population difference factor Δ_j, where j denotes the totality of quantum numbers V,J,τ of the originating state, is given by

$$\Delta_j = \frac{(2J+1)g_\tau}{Q} e^{-E_j/kT} (1 - e^{-\Delta\omega_j/kT}) \tag{8}$$

where g_τ is the nuclear spin statistical weight (=1 or 3); E_j is the energy of the originating state; $\Delta\omega_j$ is the wavelength of the transition, and the partition function Q is given by the summation

$$Q = \sum_j (2J+1)g_\tau e^{-E_j/kT} \tag{9}$$

where the summation is over all states, not transitions.

This procedure gives a value of $|\chi^{(3)}|^2$ for each value of the frequency difference $\omega_1-\omega_2$, and it would give the CARS spectrum directly if tuned, narrow-band pump and Stokes sources were employed. The experiments carried out for this contract, however, employed a broadband Stokes source whose bandwidth was 150-200 cm^{-1}, and the pump source had a bandwidth of approximately 0.8 cm^{-1}. Under such conditions, which make possible "single-shot" generation of CARS signatures, it is proper to represent the CARS signature as an incoherent addition of monochromatic source solutions (Refs. 50 and 51) which is expressible as a double convolution integral

$$I_3(\omega_3) \sim \int d\omega_1 I_1(\omega_1) \int d\omega_2 I_2(\omega-\omega_1+\omega_2) I_2(\omega_2) \left| \chi^{(3)} (\omega_1-\omega_2) \right|^2 \tag{10}$$

where I_1 and I_2 are the spectral energy densities of the pump and Stokes sources, respectively. If $\Delta\omega_2 >> \Delta\omega_1$, then (10) can be written (Ref. 51)

$$I_3(\omega_3) \sim I_1 \int I_1(\omega_3 - \Delta)\ I_2(\omega_1^{(o)} - \Delta)\ |\chi^{(3)}(\Delta)\ |^2 d\Delta \qquad (11)$$

where $I_1 = \int I_1(\omega_1) d\omega_1$, and $\Delta = \omega_1 - \omega_2$.

Sensitivity Studies

Temperature

Calculated H_2O CARS spectra are displayed in Figure (2) as a function of temperature for an assumed pressure-broadened linewidth Γ_j of 0.25 cm^{-1} and H_2O concentration of 18% in an N_2 bath. This value of Γ_j was chosen because, as will be seen later, it is consistent with the values of linewidth actually inferred from theory-experiment comparisons. It is noteworthy that even at the lowest temperatures the predicted spectrum displays considerable detail, with the peaks arising from spectral overlaps between Q-branch transitions. As the temperature is increased, higher-lying J_T states with smaller associated Raman shifts become populated, and the width of the signature increases markedly. Associated with this increasing bandwidth is sharper and more complex spectral detail. The fact that H_2O CARS spectra are so rich in spectral detail that varies strongly with temperature, even for broadband Stokes operation, makes H_2O CARS potentially attractive for thermometry when it is sufficiently abundant.

It is also interesting to note that as the temperature increases, the modulation of the spectrum near the bandhead increases. This characteristic interference minimum, which arises from the destructive interference of the background susceptibility with the real resonant part, increases with temperature because the resonant part of the susceptibility falls off more rapidly with temperature than does the nonresonant contribution. As will be seen, the presence of this spectral modulation presents the opportunity to perform H_2O concentration measurements from spectral shapes.

Linewidth

An indication of the sensitivity of predicted H_2O CARS spectra to assumed homogeneous linewidth is given in Fig. (3), where calculated pure H_2O spectra at 400 C (673 K) for various values of Γ_j are presented. Although a variation of Γ_j with Q-branch is expected, it has been neglected in these particular calculations. The sensitivity shown is not extreme, but is large enough to require more

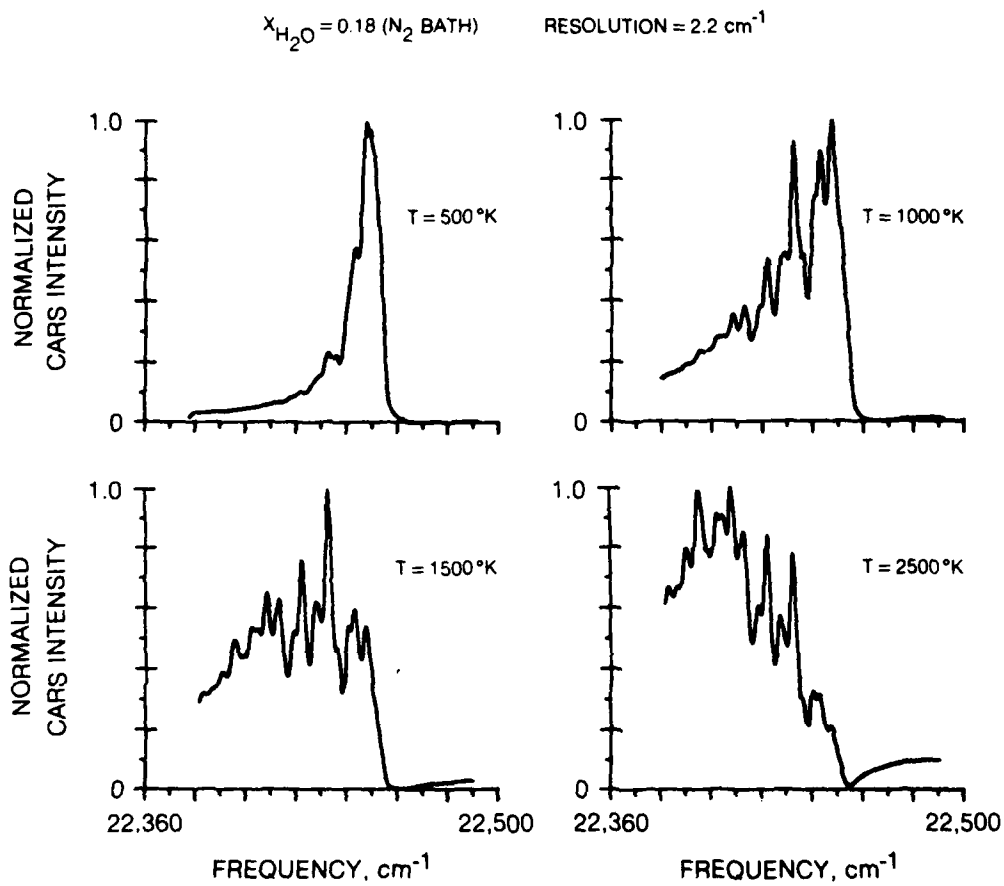

Figure 2. Calculated Temperature Dependence of H_2O CARS Spectra

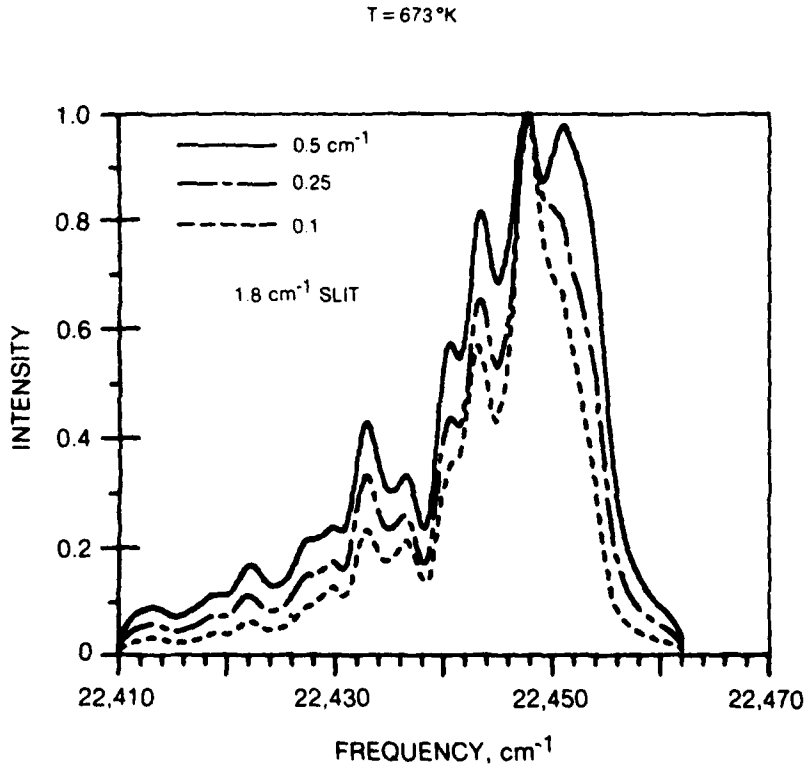

Figure 3. Effect of Raman Linewidth on H_2O CARS Spectrum

complete knowledge of these widths for very accurate work. Note that as the linewidth increases, the structure near the peak changes fairly dramatically, and the relative intensity on the "hot side" (lower frequency shifts) increases due to constructive interference effects between transitions. Also note that for this case where H_2O is a majority species there is little evidence of a nonresonant background contribution to the predicted signal.

One significant result of linewidth sensitivity studies has been that predicted spectra display surprisingly little sensitivity to the inclusion of a Q-branch dependence of linewidth. From the microwave linewidth calculations, it is known that the widths are predicted to decrease with increasing J and with increasing τ. This means, that for the Raman Q-branch transitions, the widths would be expected to decrease with decreasing Raman shift, and this effect has been simulated in computer calculations by setting the linewidth proportional to the Raman shift, so that it falls off linearly across the CARS signature.

Figure (4) compares a constant Γ_j calculation at 773 K with one in which Γ_j falls off linearly by factors of ten over the width of the signature. As seen, there is surprisingly little sensitivity of the relative features of the spectrum. The weakened constructive interference at lower shifts is apparently compensated by the fact that the integrated intensity for each isolated transition is varying as $1/\Gamma_j$. Sensitivity studies of this kind, including those corresponding to flame conditions, have led to the conclusion that the H_2O CARS spectra can be successfully described by a Q-branch-independent Γ_j that is a function of temperature and composition. In any event, deduction of a Q-branch dependence by fitting to experimental signatures would have been a prohibitively difficult task.

Concentration

As has been discussed, the modulation of the CARS spectrum, caused by interference between the resonant and nonresonant contributions to the third order susceptibility, makes it possible in certain concentration ranges to perform concentration measurements from spectral shapes. For this to be possible, the H_2O concentration must be sufficiently large that the resonant signal is not lost in the dispersionless background signal (i.e. the lower detectivity limit must be avoided) but not so large that the resonant contribution is so much larger than the nonresonant contribution that the modulation disappears. This situation is illustrated in Figure (5), where theoretical CARS spectra at T = 2000 K are displayed for various H_2O concentrations. The good concentration sensitivity of the spectra make it likely that H_2O concentration measurements can be performed from spectral shapes. At this temperature,

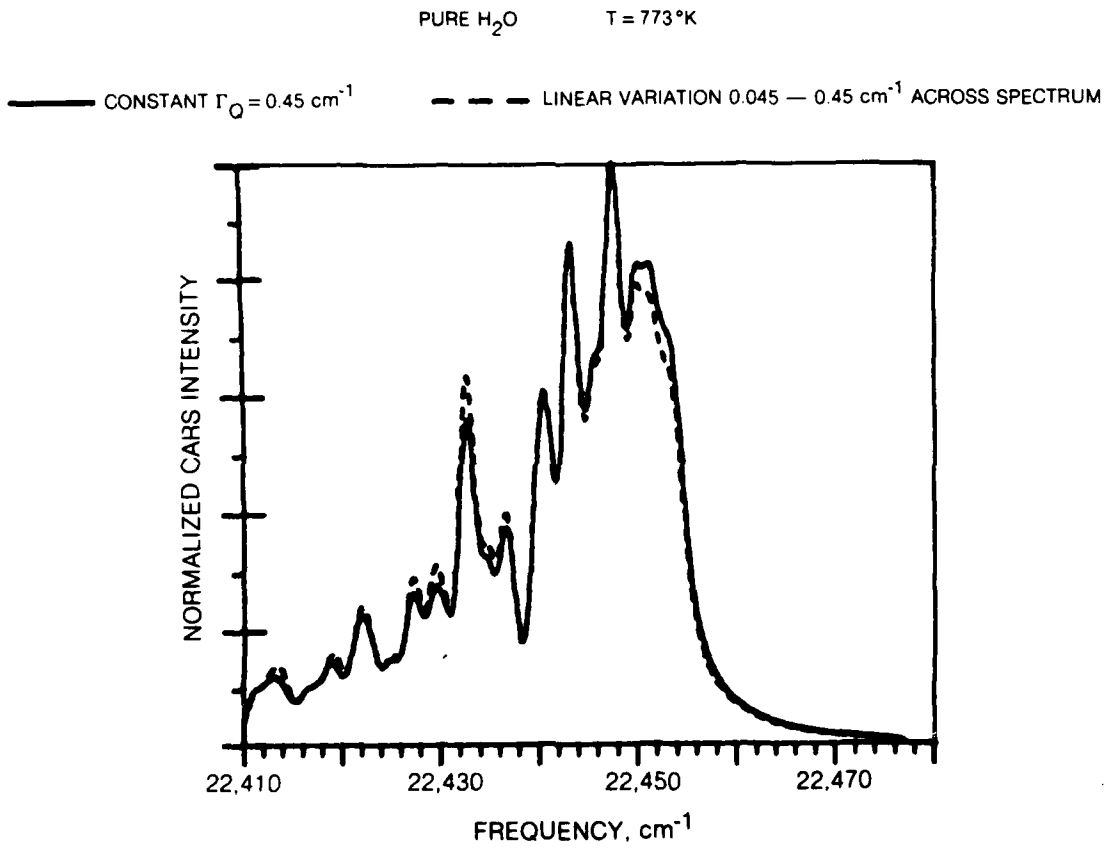

Figure 4. Sensitivity of Predicted H_2O CARS Spectrum to Q-Branch Linewidth Variation

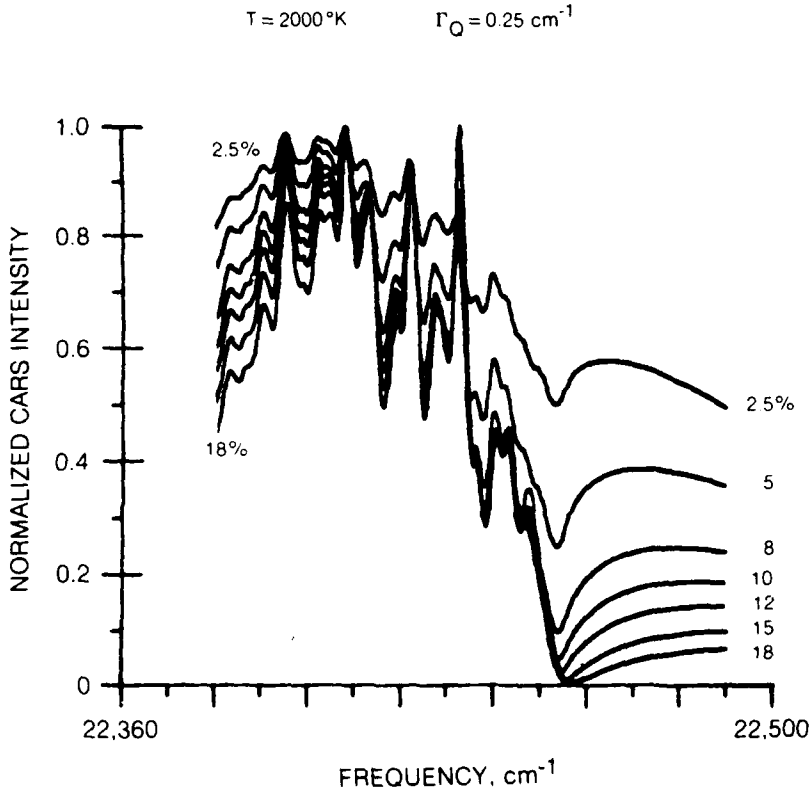

Figure 5. Concentration Dependence of Predicted H_2O CARS Spectra

the range for concentration measurement varies between roughly 2 to 20%. Sensitivity studies have shown that the modulation near the bandhead has its strongest dependence on H_2O concentration at a given temperature, with the dependence on Raman linewidth being much weaker.

For concentrations large enough that there is no measurable modulation in the CARS spectrum, the H_2O concentration must be deduced from the integrated signal intensity (suitably normalized, as previously discussed in this section). Figure 6, shows the temperature dependence of the integrated CARS intensity for pure H_2O and 50 percent H_2O in N_2. The decrease of the integrated intensity mainly reflects the decreasing density. There is a family of such curves for H_2O in various concentrations. In an experiment, the concentration is determined from the curve corresponding to the intersection of the measured temperature and the integrated signal intensity. Figure 6 is representative only of the technique because the curves were calculated for linewidths invariant with temperature.

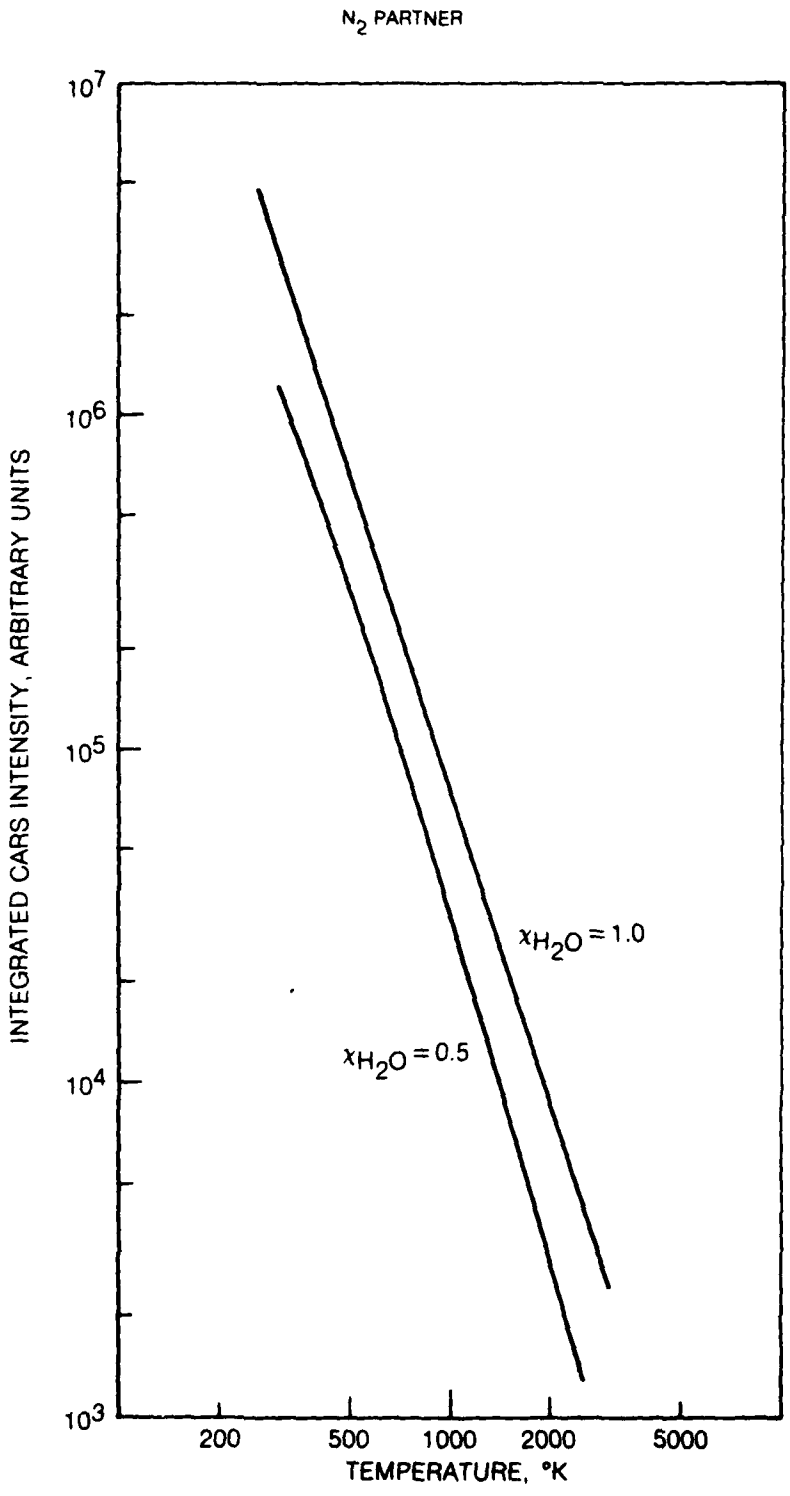

Figure 6. Calculated Dependence of Integrated CARS Intensity on Temperature

H_2O CARS EXPERIMENTS

This section begins by describing the CARS apparatus used to generate spectra of H_2O. The approach was to use collinear phase matching to maximize the CARS signal and produce the highest quality spectra for computer fitting. The heated cell used in the lower temperature range is described and some typical spectra are shown. Collinear phase matching was found to give insufficient spatial resolution for flame probing so a scheme (Ref. 5) which enhances the spatial resolution was employed. This section ends with a description of the burners that were probed. The experimental results and the theoretical predictions are compared in the section following this one.

Description of the Apparatus

The CARS apparatus used for the H_2O experiments is illustrated schematically in Fig. 7. Figure 8 shows a photograph of the apparatus. Starting with Fig. 7, a frequency-doubled Nd:YAG laser is beam split to give the primary pump beam (ω_1), and a second beam which is further split and used to optically pump, slightly off-axis, a dye oscillator and amplifier. The oscillator is operated with a flat-flat Fabry-Perot resonator fitted with broadband dielectric-coated mirrors. The dye laser output is broadband and is tuned to the desired spectral range by adjusting the concentration of the dye in the solvent solution. LD-690 (Exciton) dissolved in methanol at about 2.5×10^{-4} molar concentration was used throughout these measurements without appreciable degradation or wavelength shift. The dye solution is circulated through both dye cells, which are connected in a flow series arrangement. The dye cells are positioned at Brewster's angle so the output is nominally horizontally polarized as was the ω_1 pump. Telescopes are used in both pump and dye (Stokes) beams to make the focal spots coincident and comparable in size. The pump and Stokes beams are combined on a dichroic mirror, DM, and collinearly focused by a 20 cm focal length plano-convex lens. The laser beams and the generated CARS beam are recollimated by another 20 cm lens and sent to a dichroic mirror which was selected to reflect the 532 nm pump at > 99% reflectivity at 45° and to pass the CARS beam. A blue glass filter (GF) and a cut-off filter (COF) block the Stokes beam and any residual pump beam that pass through the dielectric mirror. The remaining CARS beam is then focussed onto the entrance slit of a homemade 1-m spectrograph equipped with a concave holographic grating (American Holographic). In this spectrograph the CARS beam passes through a horizontal ~25 micron wide slit, and expands onto the grating which vertically disperses and focuses the CARS beam at the output. The light is detected by a vidicon and stored in an optical multichannel analyzer (EGG-PARC). The dispersion at the H_2O CARS frequency was approximately 0.48 cm^{-1} per vidicon element (channel).

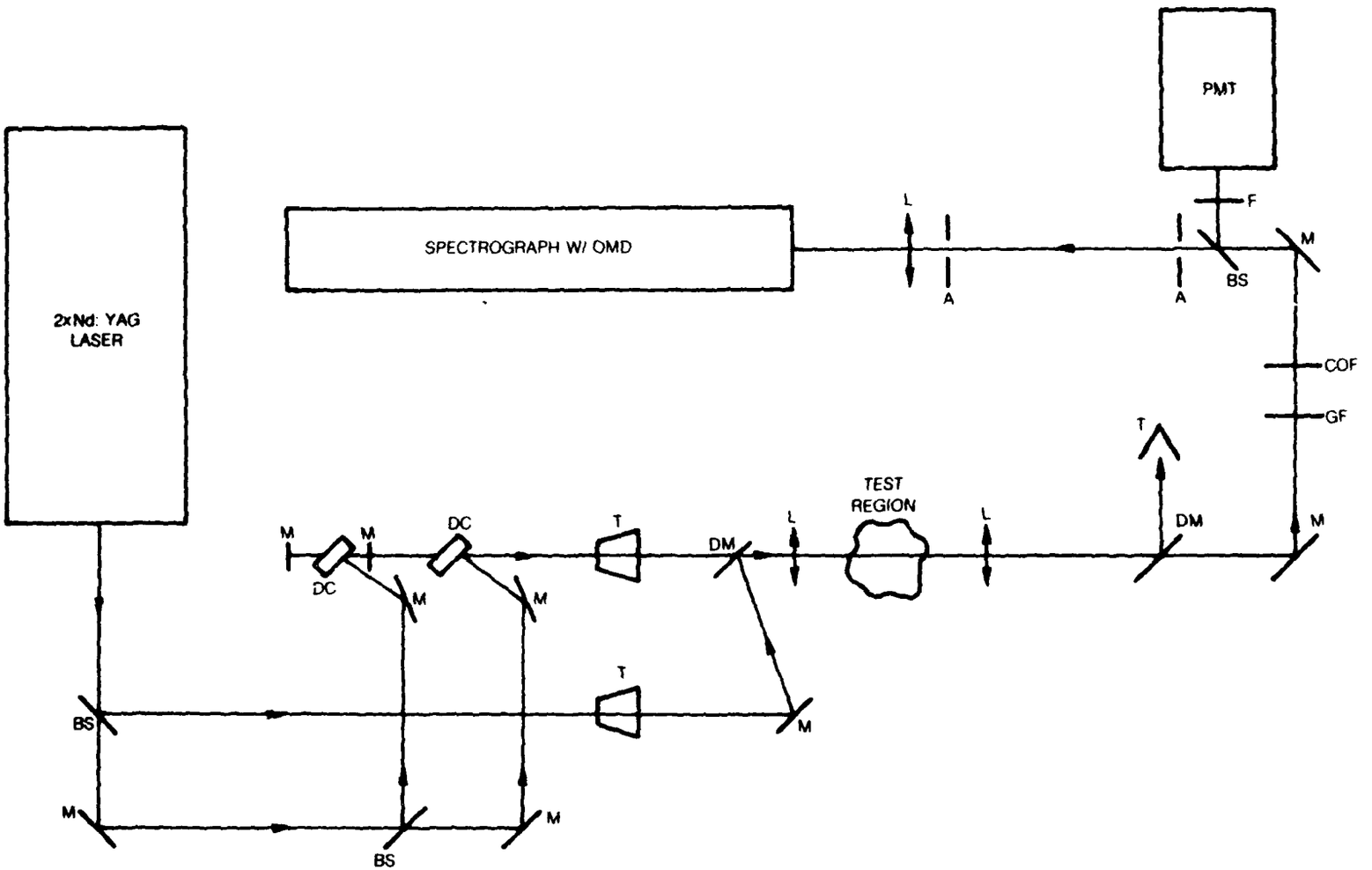

Figure 7. CARS Experimental Layout

Figure 8. H_2O CARS Experimental Apparatus

The resultant spectral resolution, determined from computer fits to the experimental data, was approximately 1.5 cm^{-1}. The data from the OMA was sent by serial interface to a DEC PDP-11/34a laboratory minicomputer and stored on a hard disk. Optical alignment of the laser beams was monitored by a photomultiplier tube viewing a portion of the CARS beam which was split off by an uncoated microscope slide. The photomultiplier is equipped with a narrow-band interference filter to reject spurious signals. This detector arrangement has a large acceptance angle and, therefore, permitted the adjustment of the pump and Stokes beam for maximum CARS signal generation.

The CARS system as configured had a pump laser energy of 30 mJ/pulse, the primary pump beam being attenuated to avoid optical breakdown in the focal volume. The focal diameter was estimated from knife edge tests to be ∿110μm. The dye laser energy was ∿ 7 mJ/pulse. The dye beam focal diameter was similarly estimated to be 60 μm. As has been stated, the spectral output of the dye was broadband, and had a bandwidth (FWHM) typically of 180 cm^{-1}.

In order to produce a H_2O mixture at known temperature and concentration, the heated cell arrangement illustrated in Fig. 9 was used. Distilled liquid water was heated in a flask to a controlled (∿ 0.2 K) temperature. A test gas was fed in below the water line, issued through a fritted glass disk and bubbled up through the heated water. The result was a saturated mixture of H_2O and the diluent gas. The experiments were conducted at one atmosphere pressure; therefore to vary the mixture from 4 to 100 percent H_2O concentration, it was required that the flask temperature be varied from 28 C to 100 C. As can be seen in the photograph, the H_2O/gas mixture was led from the flask through a heated line to the heated cell. The heated cell was cylindrical: 25 cm long and 6.4 cm diameter. It was equipped with 5 cm diameter, 1.27 cm thick quartz or glass windows, sealed with metal O-rings. The entire length of the cell was heated with special, high-temperature heating tapes. The temperature in the cell was measured by a bare iron-constantan thermocouple inserted through the wall to the center of the cell. This thermocouple was connected to a proportional temperature controller. The readout of the controller was checked against a second thermocouple, inserted through a dummy window and read with a standard bridge, and found to be quite accurate. The heated cell and heated line were operated at the same temperature, by separate heaters and controllers. After flowing through the cell, the water vapor was condensed in a tubular heat exchanger, the end of which was open to the atmosphere or could be attached to a vacuum pump, although no subatmosphere measurements were attempted. The maximum cell temperature attainable was limited by the heater power to approximately 815 K.

In addition to the heated cell, the photograph (Fig. 9) shows a second unheated cell. This cell was filled with dry N_2 at 1 atmosphere and was used

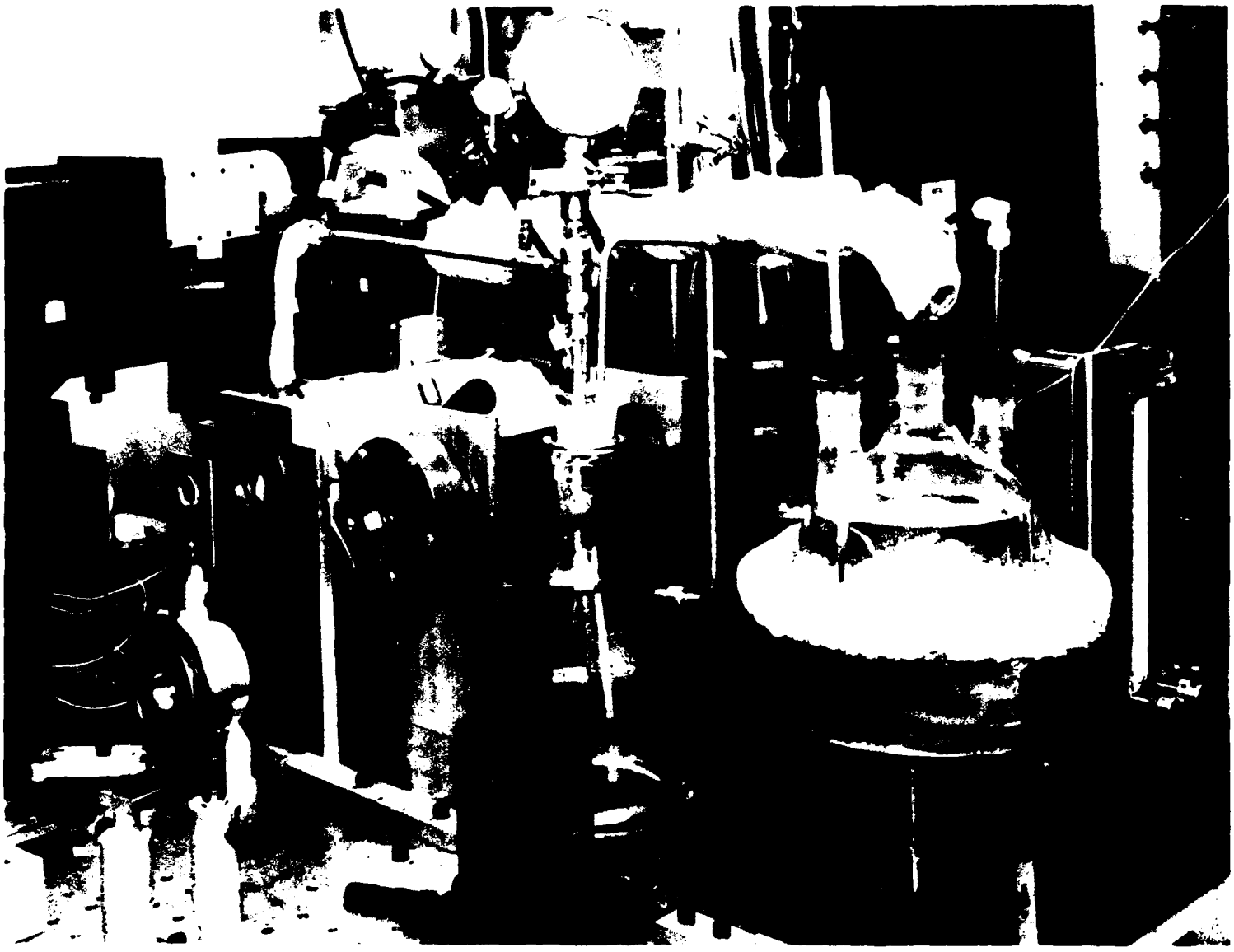

Figure 9. Heated Cell for H_2O CARS Measurement

to generate a CARS signal through χ^{nr}. This spectrum mirrored the dye laser spectrum and was used to check the dye spectral position and width. The dye laser spectral profile was recorded in this manner during each series of runs. The dye profile (fitted to a Gaussian) shape was convolved with the calculation of $\chi^{(3)}$ to model the experimental CARS profile.

H_2O CARS Measurements in the Heated Cell

The CARS spectrum of H_2O was measured in the heated cell at temperatures from 400 to 800 K, and concentrations from $\sim$ 3 to 100 percent. A number of diluent gases were used including N_2, CO_2, Ar and He. Nitrogen, since it is the most abundant component in air-fed combustion, was investigated most thoroughly. The effect of CO_2 is important because it too is present in abundance in hydrocarbon-fueled combustion products. Argon was studied to see the effect of a monatomic species; and helium was employed to minimize the nonresonant contribution to the CARS spectrum when the H_2O concentration was small.

The data stored on a typical data file are represented in Fig. 10, where the CARS spectrum of H_2O at 30 percent concentration in N_2 at a cell temperature of 673 K is plotted. The abscissa is proportional to frequency and increases to the right. The dispersion of the spectrograph in this region corresponds to 0.48 cm^{-1}/channel. This particular spectrum represents an average of 500 laser pulses (50 secs), and the CARS beam has been attenuated to avoid saturation of the vidicon target with neutral density filters with total optical density of 2.52.

The effect of temperature on the H_2O CARS spectrum is illustrated in Fig. 11 for a 12 percent H_2O mole fraction in N_2. This mole fraction represents a value typical of the post flame H_2O concentration in hydrocarbon combustion. The spectra have been plotted with a digital plotter and the axis labels have been suppressed. The spectral intensity is in arbitrary units because each spectrum represents a different number of pulses, and different attenuation. The shift of the population to increase the contribution of Q branch transitions of smaller frequency shift is clear.

Figures 12 and 13 show the effect of H_2O concentration on the spectrum at 473 and 773 K respectively. The modulation due to the background nonresonant susceptibility is seen at the lowest concentration. This modulation disappears between 12 and 15 percent at the lower temperatures of the cell data. Another effect is more apparent in the hotter spectra (Fig. 13). A feature that is just a shoulder in the bandhead region at low concentration emerges to a prominent peak at high concentration. This effect was observed in the linewidth sensitivity studies and is examined in more detail in the next section which compares theory and experiment.

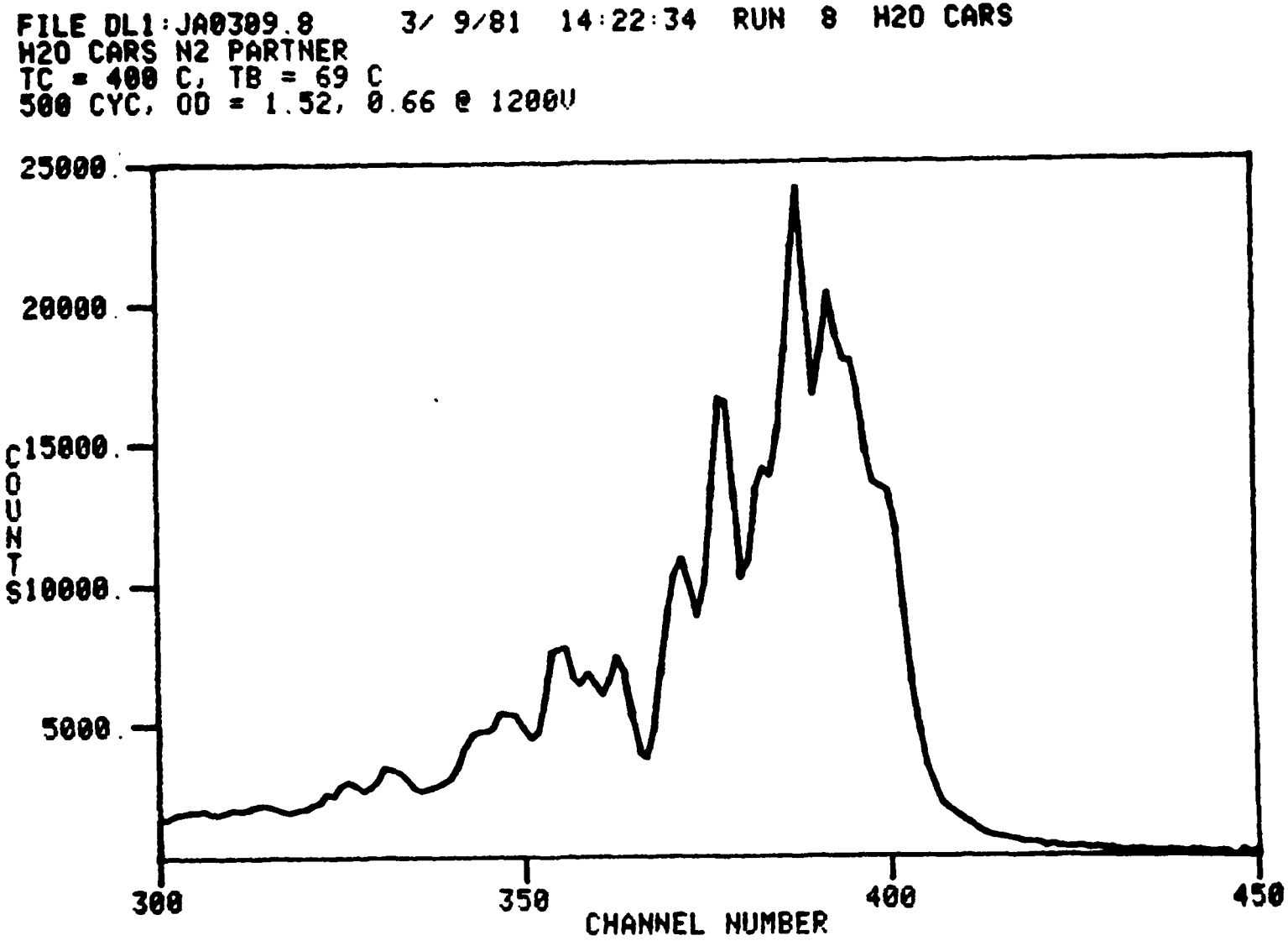

Figure 10. Typical H_2O CARS Data File

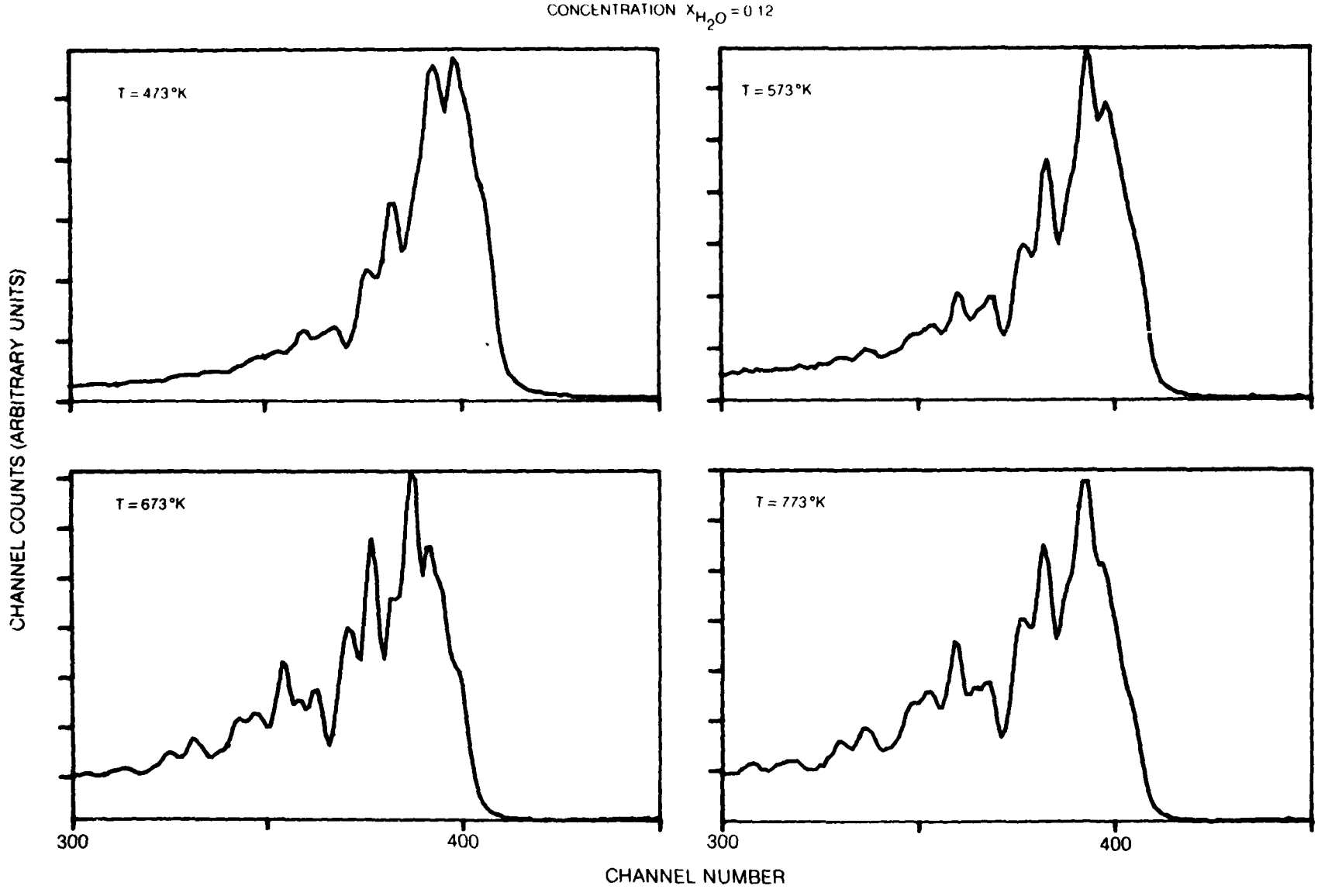

Figure 11. Effect of H_2O Temperature on Experimental Spectra — N_2 Partner

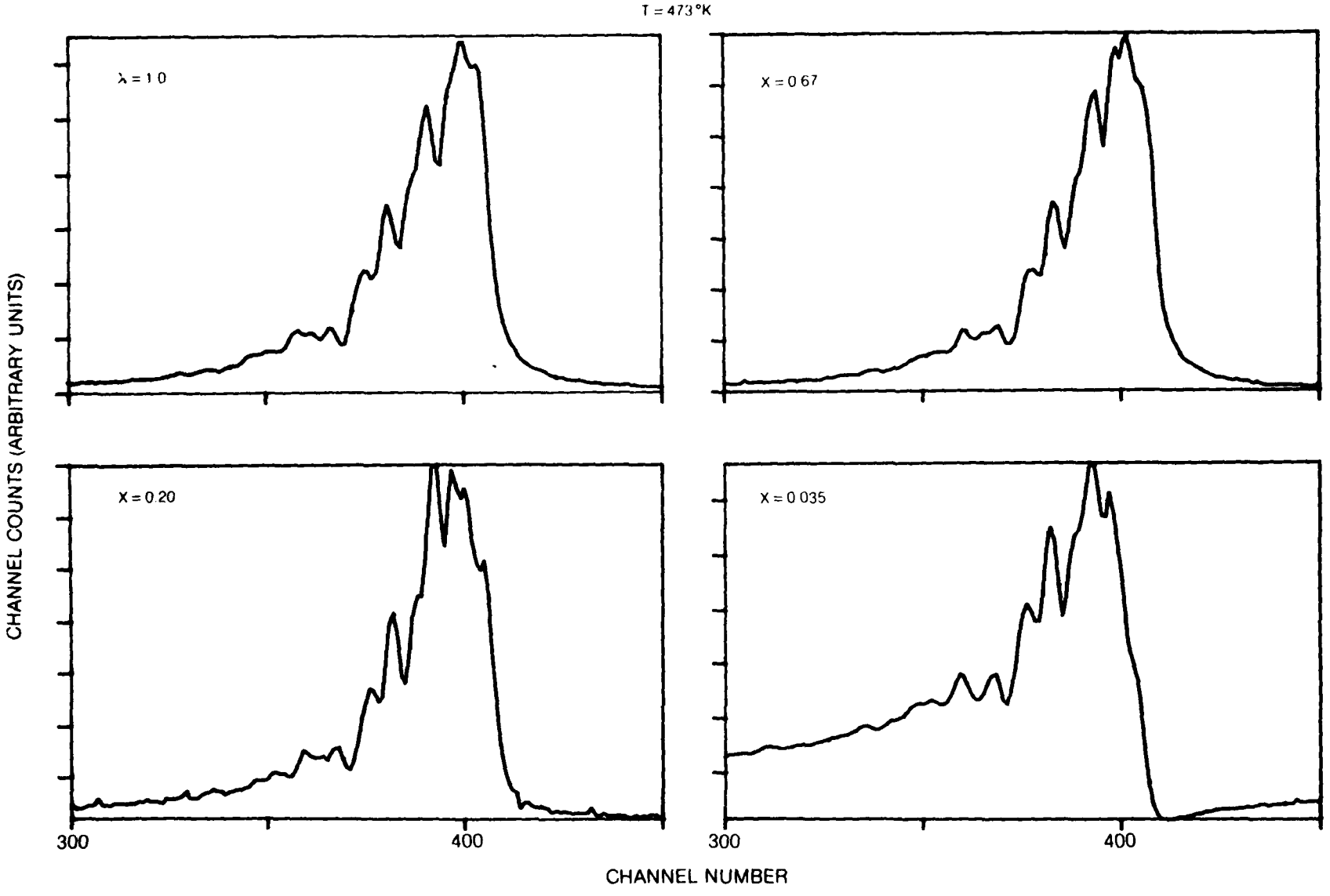

Figure 12. Effect of H_2O Concentration on Experimental Spectra — N_2 Partner

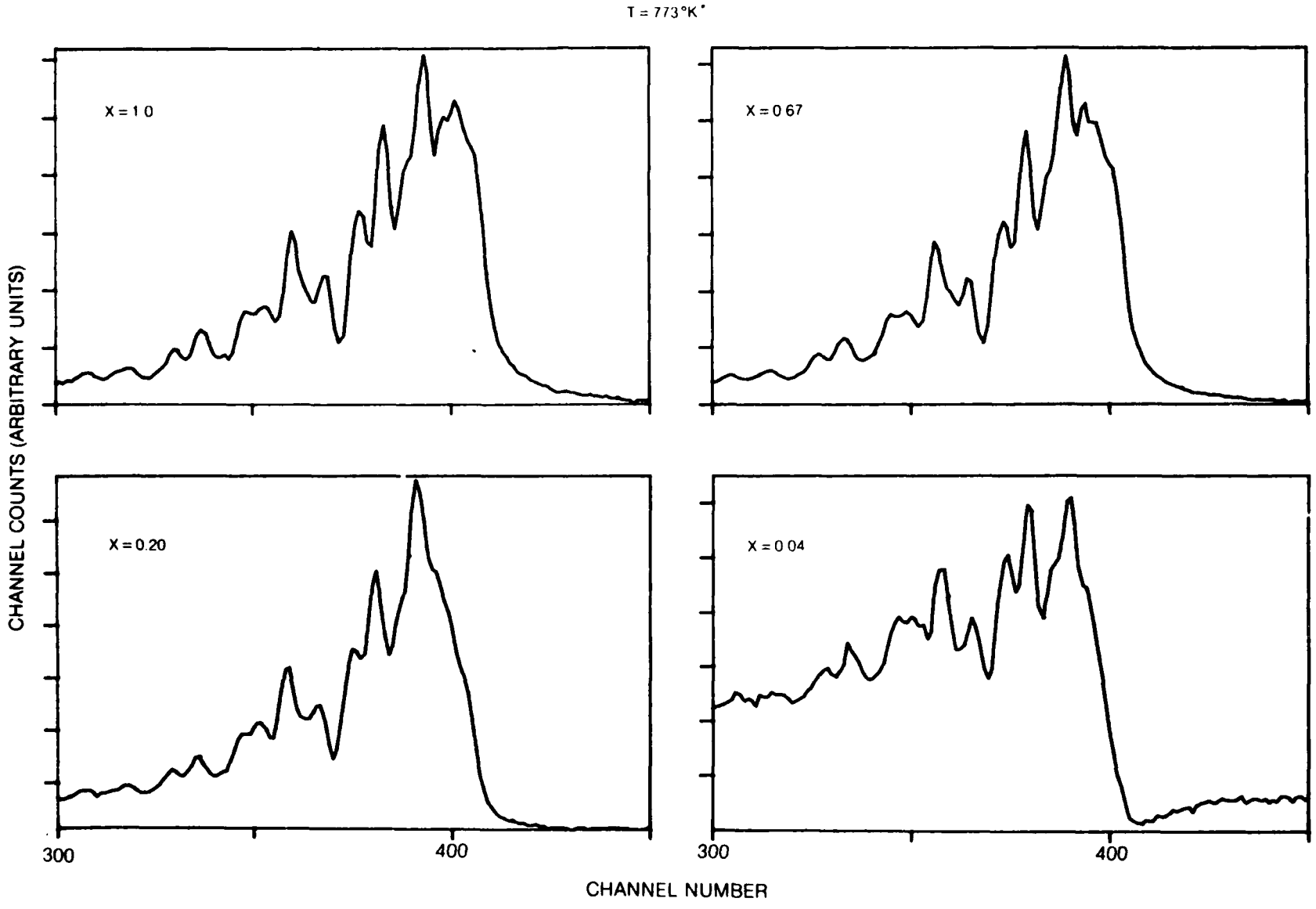

Figure 13. Effect of H_2O Concentration on Experimental Spectra — N_2 Partner

Figure 14 shows the effect of collision partner on the CARS spectrum at 773 K and approximately 7.5 percent H_2O. The helium spectrum is modulation free because of its small nonresonant susceptibility (Table 1). N_2 and Ar are nearly comparable with the argon modulation slightly higher as would be expected. CO_2 produces the largest modulation and has the largest $_{nr}$ of the group. The actual H_2O concentration for He, N_2, CO_2 and Ar collision partners are 7.5, 7.6, 7.7 and 6.0 percent respectively, but these variations don't affect the general observations.

H_2O CARS Measurements in Flames

In addition to the heated cell measurements, CARS measurements of H_2O were made in CH_4-air flames. The burners were premixed and stabilized on a bundle of many small diameter tubes. Burners with diameters of 2.54 and 7.6 cm were used. Both burners were operated at the same stoichiometric flowrates. Higher velocities in the smaller burner gave lower heat transfer losses and higher volumetric heat release and consequently, a higher temperature. The temperature measured at the center of the burner was 2070 and 1670 K for the 2.54 cm and 7.6 cm diameter burners, respectively. This temperature was measured with a 0.3 mil Pt-Pt/10% Rh thermocouple that was coated with yittrium oxide and calibrated against Na line reversal measurements. Thermocouple measurements revealed that the smaller burner exhibits a central hot core surrounded by a cooler outer region. The temperature drops ~ 100 K in the central core, $r/r_o < 0.5$. CARS measurements with collinear phase matching seem to reflect this result in that the experimental spectrum appeared to be colder than the spectrum calculated from the temperature measured on the central axis. To minimize the effects of spatial inhomogenity on the measured spectra, a three-dimensional phase matching scheme was used (Ref. 5). The frequency-doubled Nd:YAG laser operates with an unstable resonator cavity and produces an annularly-shaped beam. To achieve higher spatial resolution, this pump was expanded and the dye laser was contracted slightly; so that, if the profile of the two beams was examined at the lens focussing into the flame, the dye laser beam would be observed to be fully within the hole in the annulus. That the CARS beam is generated in a annular ring, as it should be, was confirmed by blocking the center of the CARS observation optics without appreciably degrading the CARS signal. With this modification, the data, to be presented, agree with calculations.

The measurements in the flames will be presented with the comparisons with calculated spectra in the following section. That section also compares calculations with the heated cell measurements.

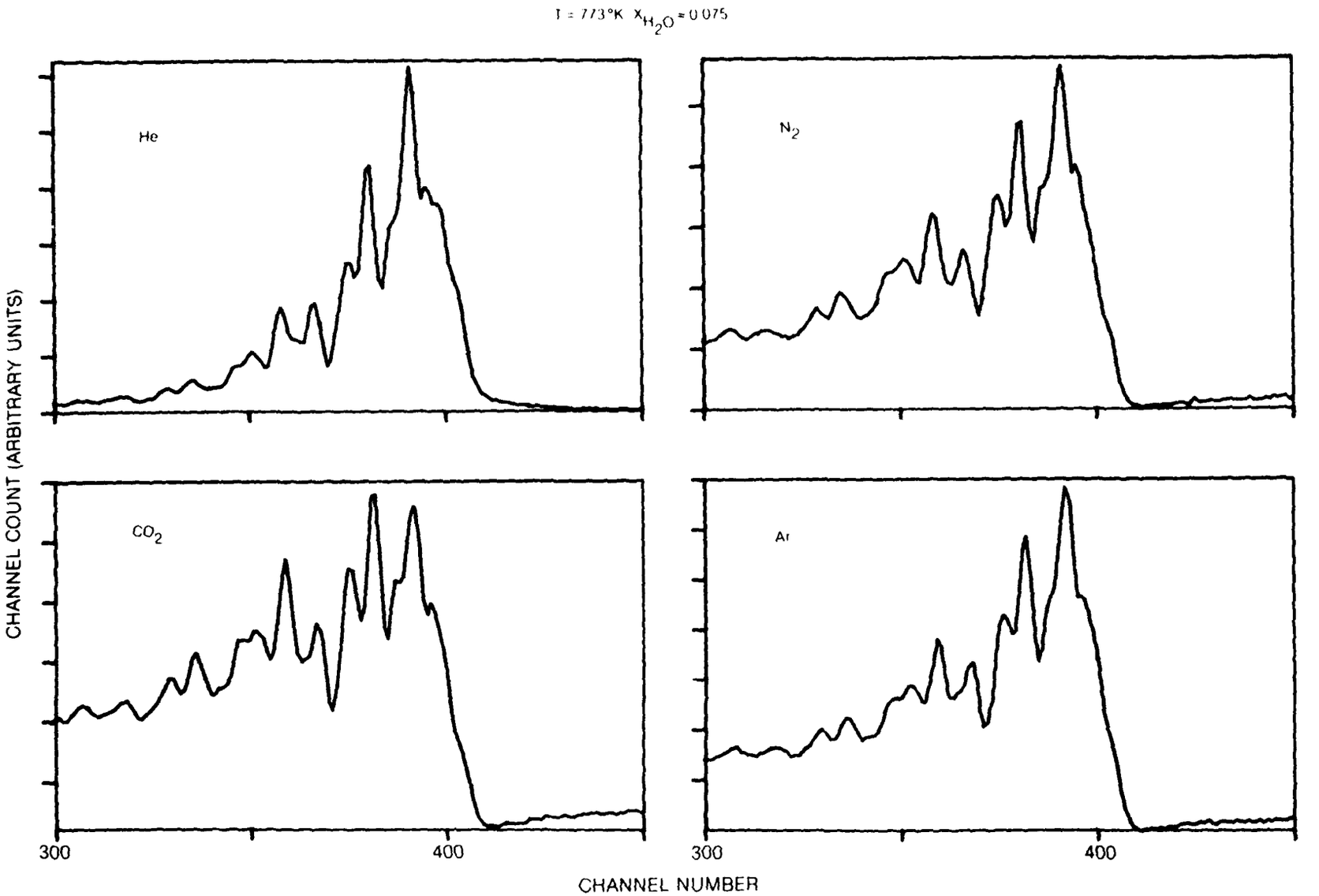

Figure 14. Effect of H_2O Collision Partner on Experimental Spectra

COMPARISON OF EXPERIMENTAL AND CALCULATED H_2O CARS SPECTRA

The results of the experiments and the CARS computer code calculations are compared and discussed in this section. Raman linewidths and broadening parameters for N_2, CO_2 and self collisions are inferred from the heated cell measurements by least-squares fitting to calculations. Only a portion of the nearly seventy experimental spectra were analyzed because of the time required to fit spectra; nevertheless, the collision partners relevant to combustion were considered. The burner spectra were also analyzed, but the range of conditions is necessarily limited by the range of conditions available in the post-flame region of premixed flames.

Data Reduction

Analysis of the experimental CARS signatures was carried out using a least-squares fitting routine developed previously under corporate sponsorship. The program, which uses Marquardt interpolation to minimize a sum of squares, is, in principle, capable of handling multiple fitting parameters, but, for the cases run under this contract, these were restricted to two: the Raman linewidth and a scale height factor. The program as used in this contract stores calculated CARS spectra as a function of the Raman linewidth in tabular form; for values of the linewidth not equal to the discrete values contained in the tables, the CARS spectra are supplied to the fitting routine by interpolation. This interpolation approach using previously tabulated spectra makes it possible to consider only one physical fit parameter besides the scale height variation. If it is economically feasible, the spectral values required by the fitting routine can be generated by having the fitting routine exercise the computer program which generates the CARS spectra. In this way, knowing the Raman linewidths, one could simultaneously determine temperature and H_2O concentration by least-squares fitting.

Test Cell Data

Because not all of the experimental signatures developed under the contract could be reduced, attention was focussed on those signatures which would be likely to yield information about linewidth that would be most useful for combustion applications. Thus, information on the Raman linewidth broadening by H_2O, N_2, and CO_2 was sought. Thus, for the test cell data, the pure H_2O signatures were analyzed at each of four temperatures: 473, 573, 673, and 773 K. For the N_2 dilution experiments, the signatures corresponding roughly to 3.5%, 30%, and 50% H_2O in N_2 background were reduced. The corresponding pure N_2 contribution to the linewidth was then determined from the relationship

$$x_{N_2} \Gamma_{H_2O-N_2} = \Gamma_Q - (1 - x_{N_2}) \Gamma_{H_2O-H_2O} \qquad (12)$$

where Γ_Q is the best fit Raman linewidth, x_{N_2} is the mole fraction of N_2 and $\Gamma_{H_2O-H_2O}$ is the Raman linewidth for H_2O self-broadening determined from the pure H_2O experiments. Two signatures, at 473 and 773 K, corresponding to roughly 5% H_2O in a CO_2 bath, were also reduced, making a total of 18 test cell cases. In addition, three air-methane flame signatures were reduced, for a total of 21 least squares fits.

The four pure H_2O fits to experiment are shown in Figures (15-18), together with the inferred Raman linewidths. As can be seen, the theory-experiment fits are all quite good, and, as expected, the inferred Raman linewidths are relatively large and have an inverse temperature dependence. When the fact that these temperatures are all well above room temperature is taken into account, it becomes apparent that these linewidth values are not inconsistent with the microwave linewidths calculated by Benedict and Kaplan (Ref. 40).

Two signatures at 573 and 673 K corresponding to 30% H_2O in an N_2 bath are shown in Figures 19 and 20. Again, the theory-experiment agreement is very good for the best fit linewidth parameter shown. At the 30% H_2O level, there is no evidence of interference from the background nonresonant susceptibility. For these cases, the value of $\Gamma_{H_2O-N_2}$ is about 0.165 cm^{-1} atm^{-1}, which is again a number consistent with the Benedict and Kaplan calculations (Ref. 40).

Two signatures at 473 and 673 K for a water concentration of 3.5% in N_2 bath are shown in Figures 21 and 22. For an H_2O concentration this low, there is appreciable interference between the resonant and nonresonant contributions, as is evidenced by the interference minimum near the bandhead. The N_2 contribution to the Raman linewidth for these cases is again determined to be in the vicinity of 0.17 cm^{-1} atm^{-1}.

The efficiency of CO_2 as a broadening partner has been examined by reducing two signatures, shown in Figures 23 and 24. The test cell temperatures for these cases are 473 and 773 K, and correspond to water concentrations of 5.6 and 5%, respectively in a CO_2 bath. As seen, the fits to experiment are very good, and the best fit linewidth values are not greatly different from those inferred in Figures 21 and 22 for H_2O dilute in N_2. When the H_2O-H_2O contribution to the linewidth is subtracted, the conclusion is that CO_2 has just about the same broadening efficiency as N_2.

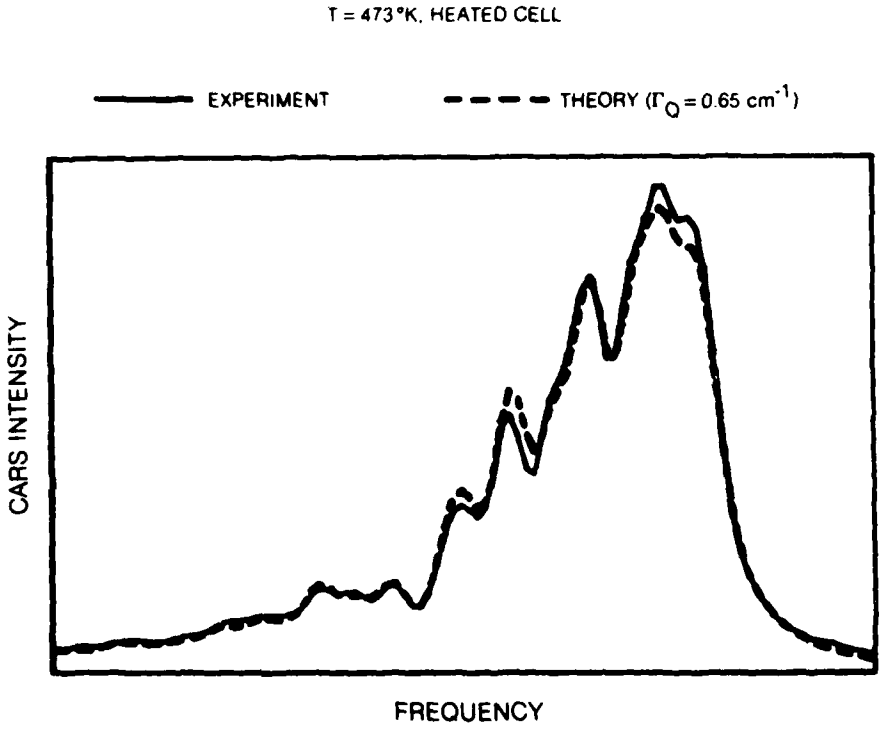

Figure 15. Comparison of Theory and Experiment — Pure H_2O

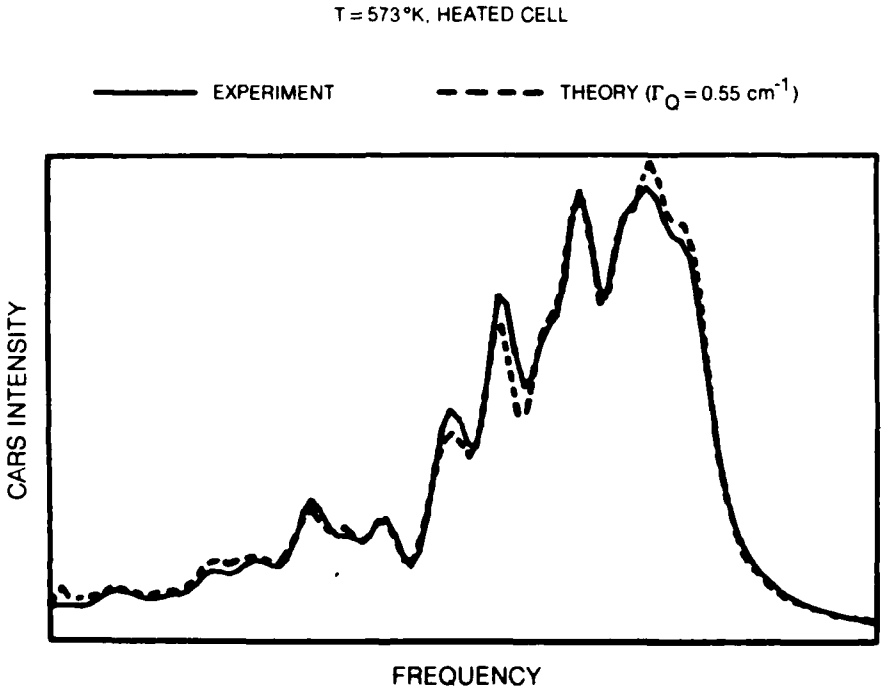

Figure 16. Comparison of Theory and Experiment — Pure H_2O

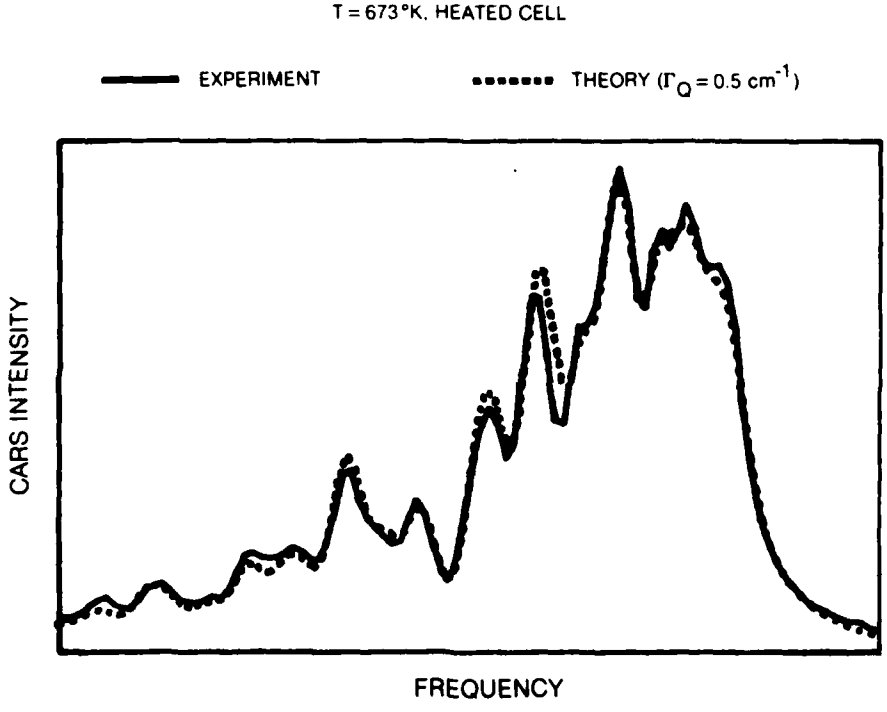

Figure 17. Comparison of Theory and Experiment — Pure H_2O

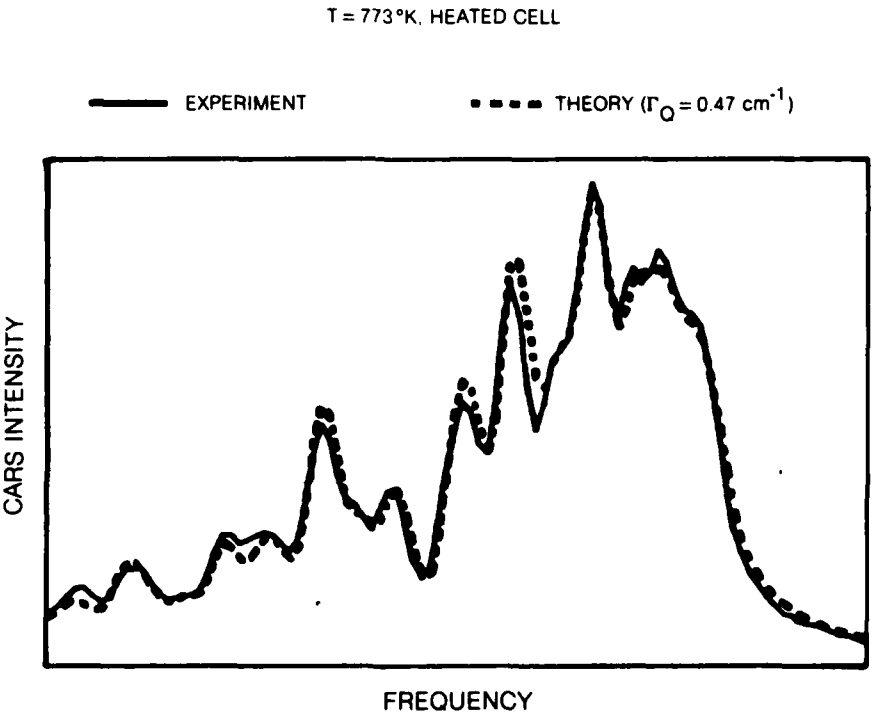

Figure 18. Comparison of Theory and Experiment — Pure H_2O

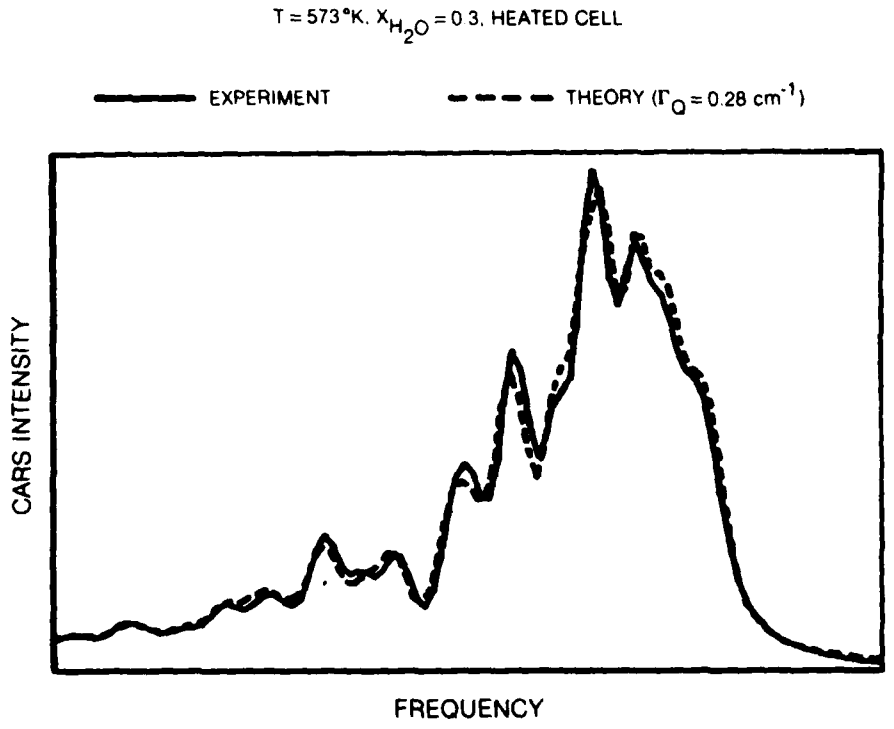

Figure 19. Comparison of Theory and Experiment — N_2 Partner

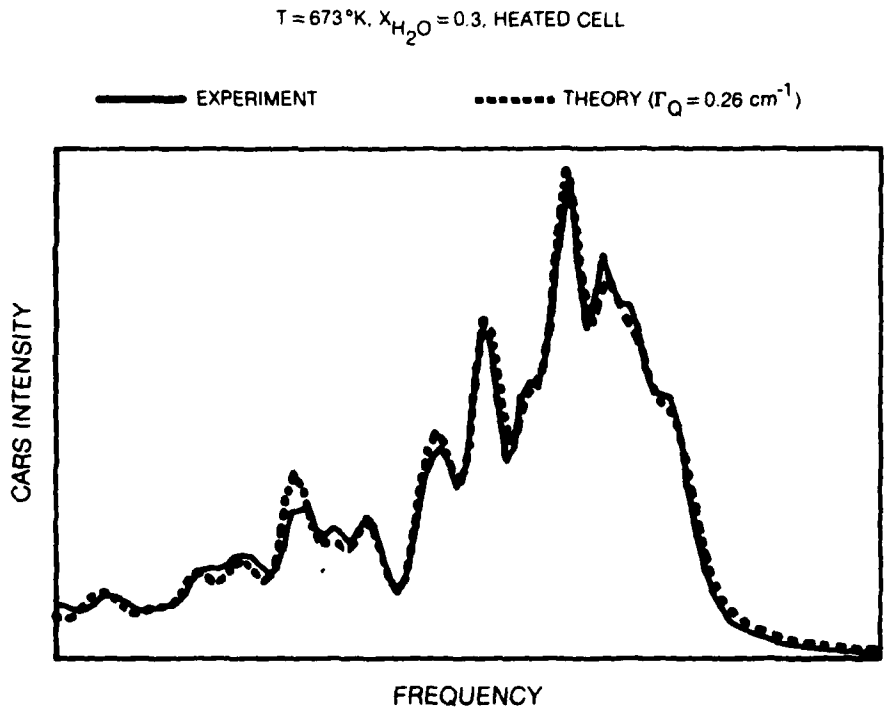

Figure 20. Comparison of Theory and Experiment — N_2 Partner

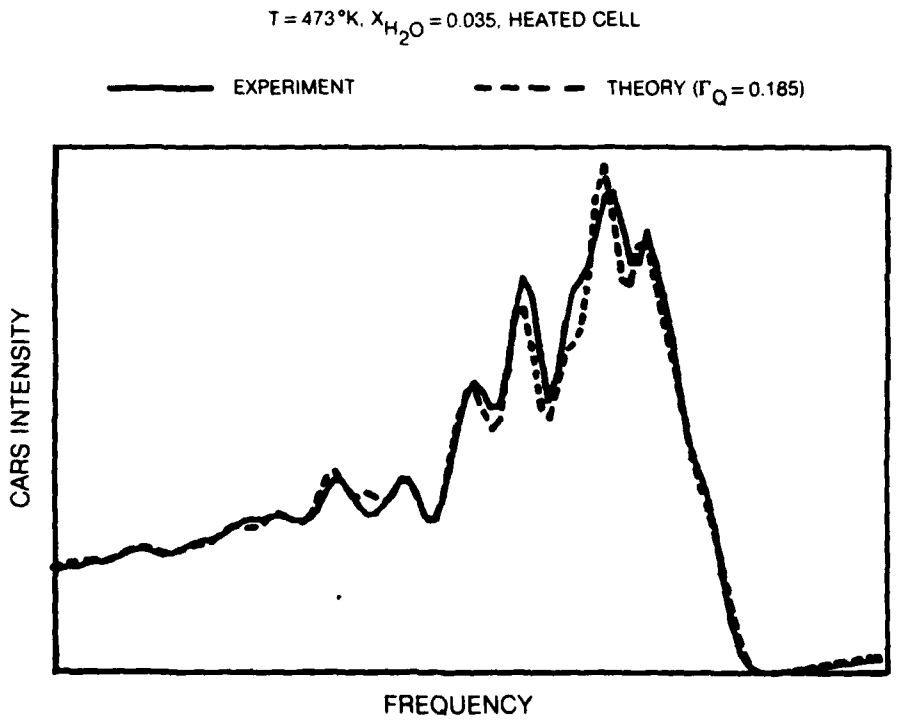

Figure 21. Comparison of Theory and Experiment — N_2 Partner

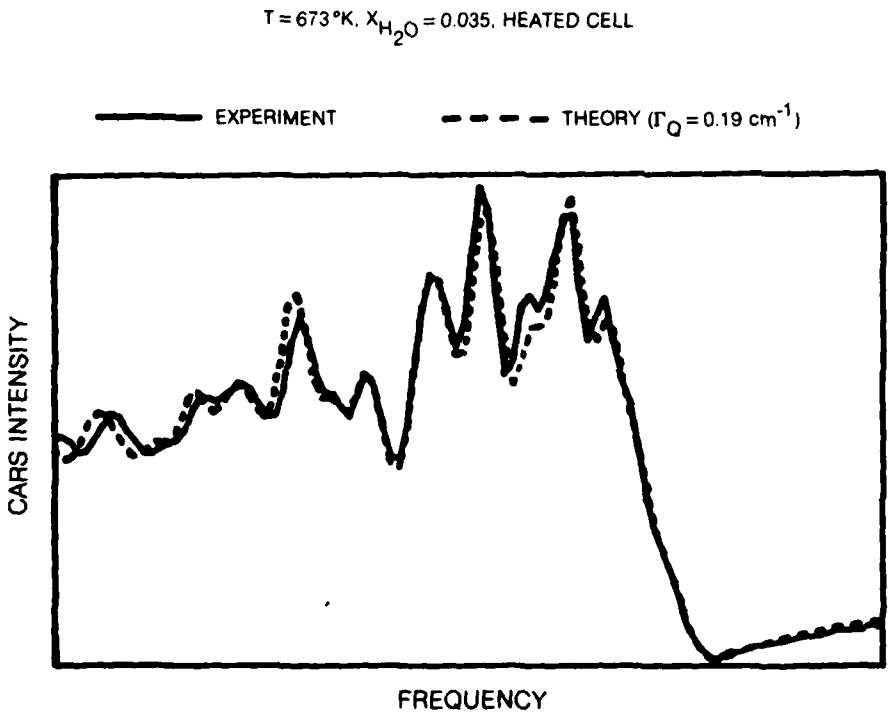

Figure 22. Comparison of Theory and Experiment — N_2 Partner

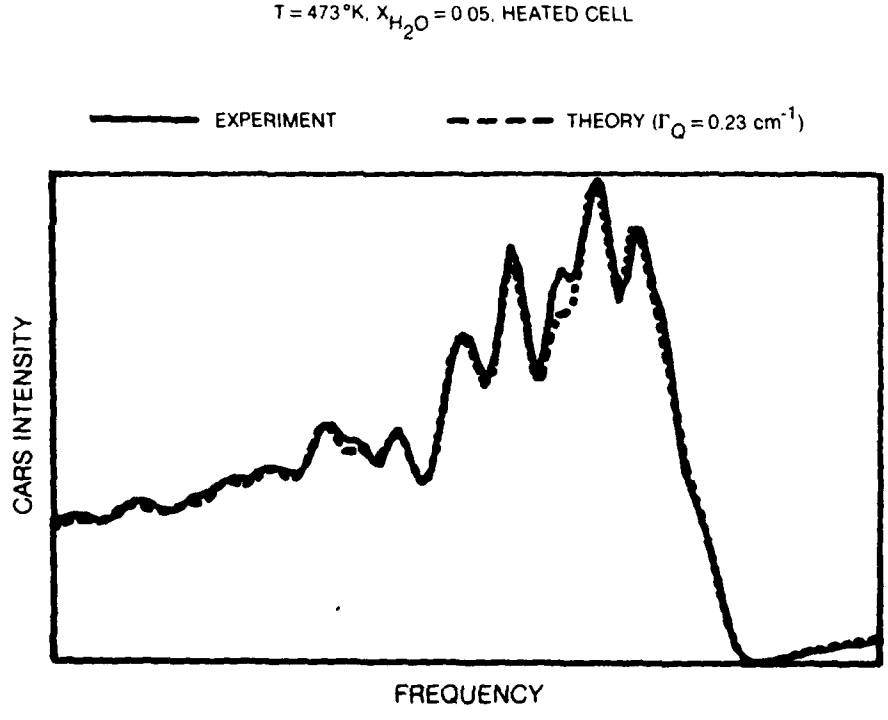

Figure 23. Comparison of Theory and Experiment — CO_2 Partner

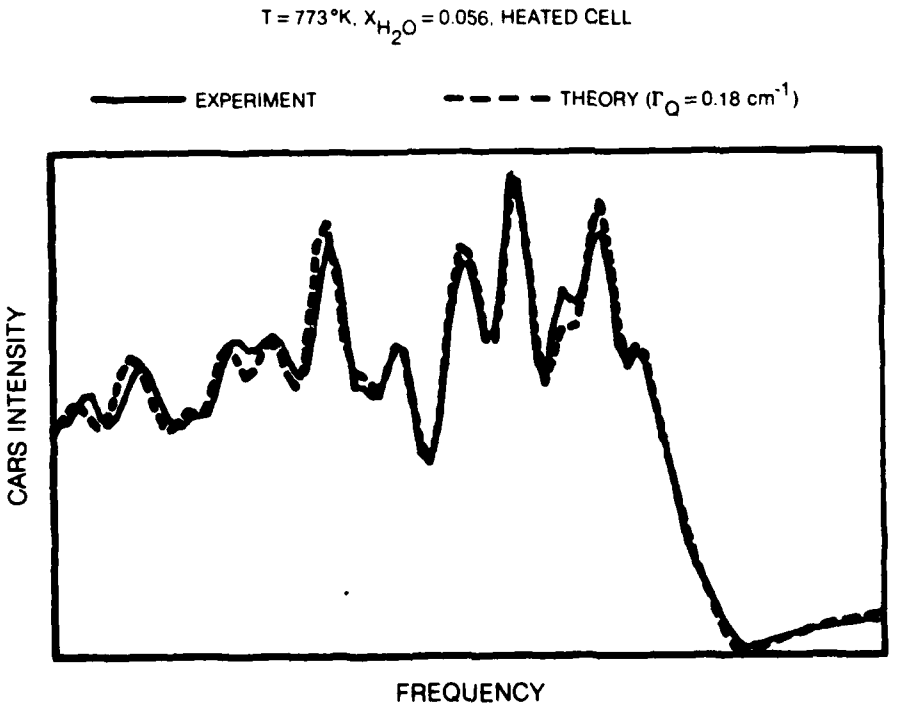

Figure 24. Comparison of Theory and Experiment — CO_2 Partner

The inferred Raman linewidths for all of the test cell data are shown in Figure 25. The H_2O self-broadening linewidths are denoted by the dark circles; and those for CO_2 broadening of H_2O by the triangles. As seen, an inverse temperature dependence is indicated for H_2O self-broadening, although the dependence seems to have become quite weak at 773 K where the broadening coefficient is about 0.5 cm^{-1} atm^{-1}. It is apparent too that broadening by N_2 and CO_2 is much less effective than H_2O self-broadening, but the indicated temperature dependence is quite weak. While there is some scatter in the values of H_2O-N_2 linewidth inferred from the various mixtures, the data would suggest a value of about 0.17 cm^{-1} atm^{-1} that is sensibly independent of temperature over the temperature range 473 to 773K. To a good approximation CO_2 can be assigned a broadening efficiency equal to that of N_2.

Flame Data

High temperature data from both the 7.6 cm and 2.5 cm diameter burners were analyzed. In the calculations, a stoichiometric composition of 18% H_2O, 9% CO_2, and 73% N_2 was nominally assumed, and the temperature was assumed to be equal to the thermocouple temperature.

For the 7.6 cm diameter burner, spectra obtained using both collinear phase matching and the three-dimensional phase matching technique were analyzed, as shown in Figures 26 and 27, respectively. The best fit linewidths in each case are about the same 0.24 and 0.25 cm^{-1}, respectively. The collinear phase matching spectrum appears colder even though the temperature is about the same ($\sim$1670 K) because of a substantial shift in dye center frequency. While there are a few points of discrepancy in the spectrum, it is fair to say that the agreement between theory and experiment is very satisfactory.

For the 2.5 cm diameter burner, only the 3-D phase matched experiments were reduced, because the collinear phase matching experiments showed evidence of insufficient spatial resolution. A theory-experiement fit to the 2.5 cm burner data is shown in Figure 28. Again, with a few exceptions, the agreement between experiment and theory is very good, and the best fit linewidth, 0.25 cm^{-1} is about the same as was inferred for the lower temperature 7.6 cm burner. The potential usefulness of H_2O CARS for thermometry is indicated by the dramatic increases in intensity on the hot side (lower frequency) as compared to the 7.6 cm 3-D phase matched spectrum. Also, the substantial degree of modulation that exists due to nonresonant background interference is to be noted; the presence of this modulation at the assumed 18% concentration of H_2O means that H_2O concentration measurements can be performed from spectral shapes in hydrocarbon-fueled flames.

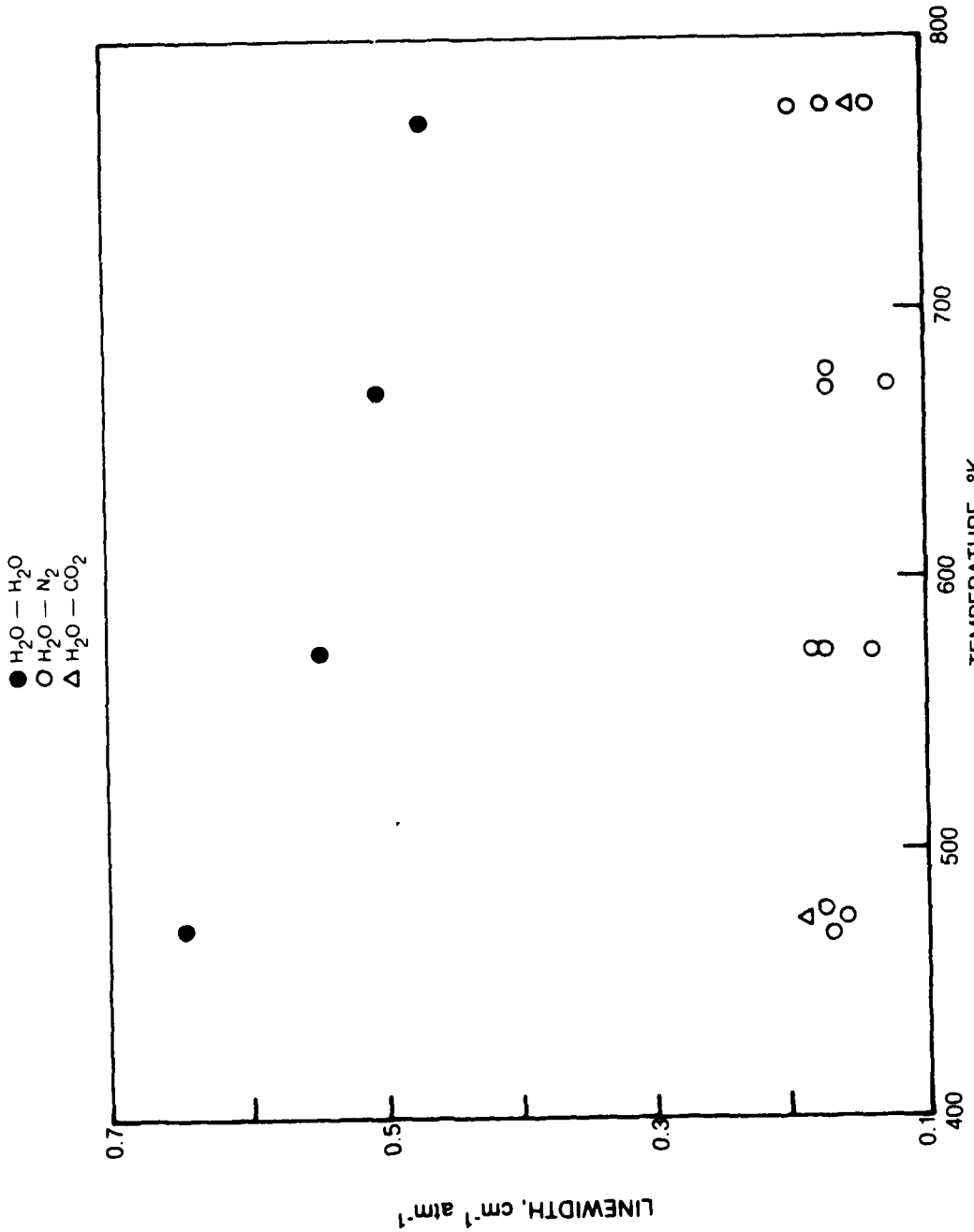

Figure 25. Summary of Test Cell Linewidth Data

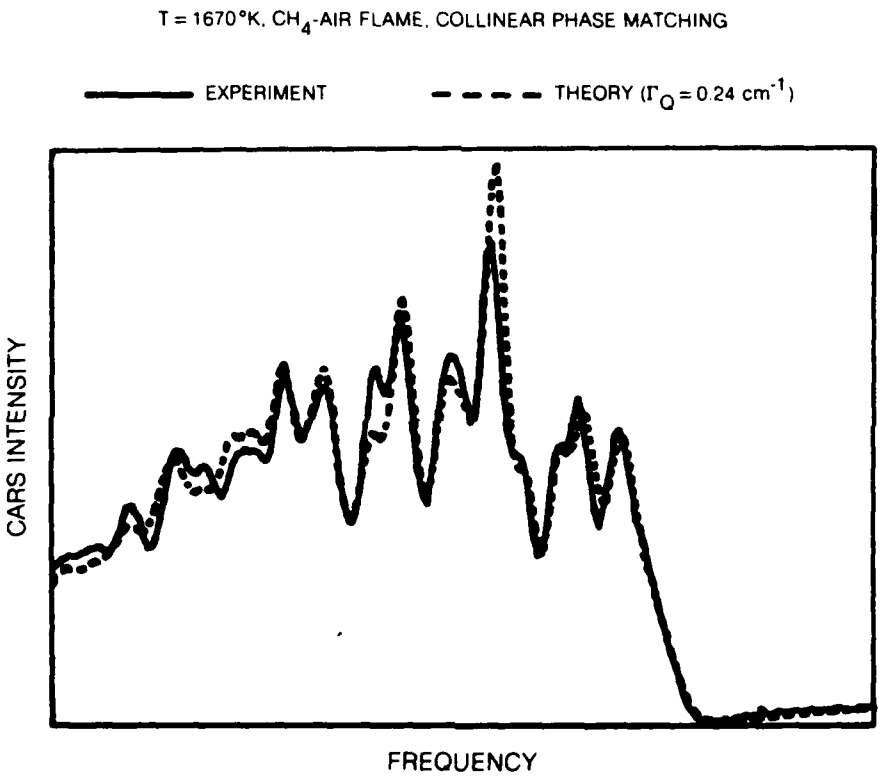

Figure 26. Comparison of Theory and Experiment

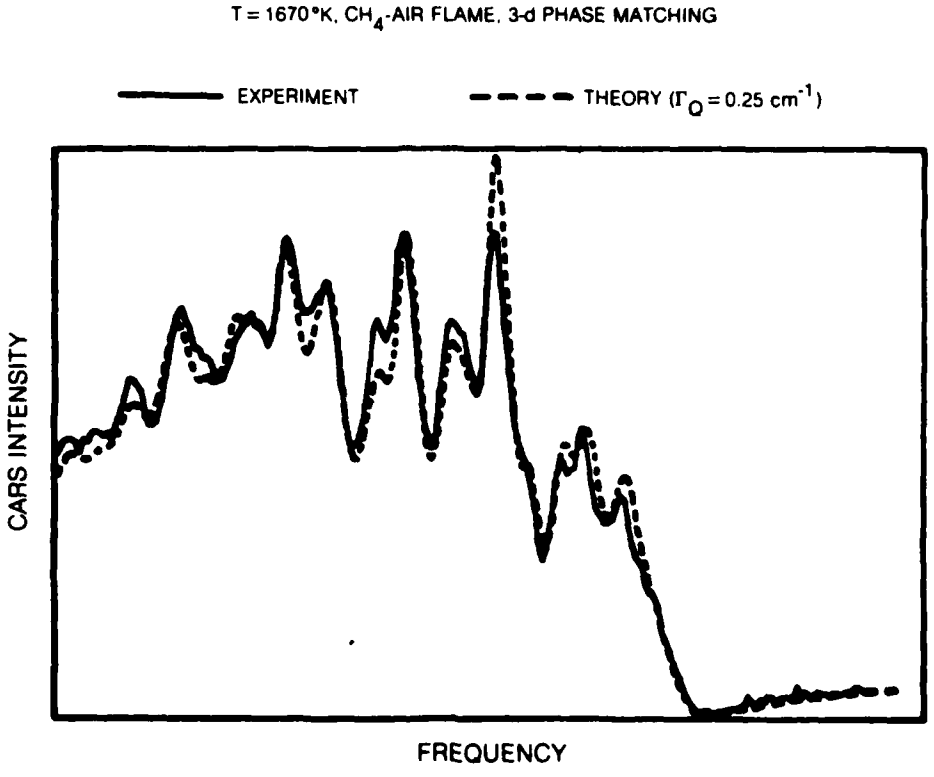

Figure 27. Comparison of Theory and Experiment

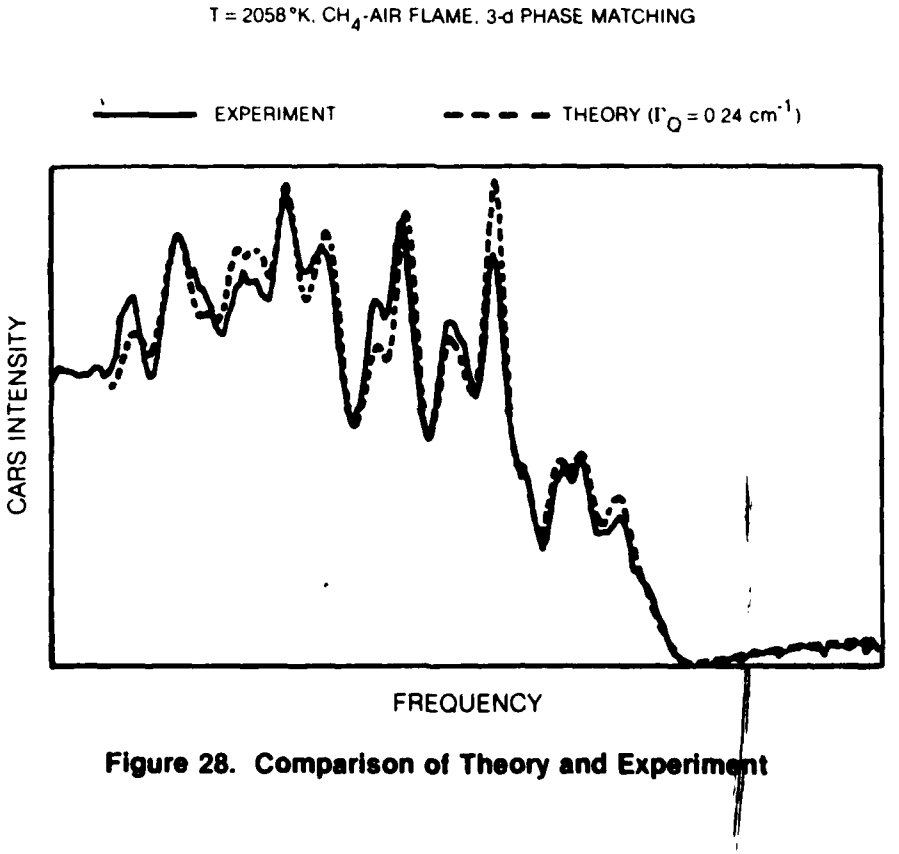

Figure 28. Comparison of Theory and Experiment

The Raman linewidths inferred from the flame measurement are roughly consistent with the results obtained in the test cell. However, from the hottest test cell data (773 K) to the flame data there is a gap of nearly 1000 K, and it is not certain how the test cell data should be extrapolated over this temperature interval. If one assumes that the N_2 and CO_2 contribution of 0.17 $cm^{-1}atm^{-1}$ can be extrapolated out to flame temperatures, and that the H_2O broadening contribution has leveled off in the vicinity of 0.40 $cm^{-1}atm^{-1}$, then the mixture-weighted linewidth one would expect at flame temperatures would be about 0.22 cm^{-1}, a value not far from the 0.24-0.25 cm^{-1} actually obtained in the methane-air flames. The analysis of the flame data, therefore, indicates that a nearly temperature-independent linewidth value of 0.24-0.25 cm^{-1} atm^{-1} be used for stoichiometric mixtures. For non-stoichiometric mixtures, a good approximation to computing the appropriate mixture-weighted linewidth might be to assume that the contribution of H_2O self-broadening to the linewidth is about 2.5 times that of the diluent molecules N_2 and CO_2, which would give the following approximate expression for the mixture-dependent Raman linewidth at flame temperatures:

$$\Gamma_Q \simeq 0.3x_{H_2O} + 0.2 \qquad (13)$$

The results of the theoretical fittings to the experimental signatures can be summarized by saying that for test cell conditions, the understanding of the temperature and concentration dependences of the H_2O Raman linewidths is now sufficient to permit accurate H_2O thermometry and/or concentration measurements. At flame conditions, the inferred Raman linewidths are consistent with the test cell results, but the temperature gap separating the test cell and flame results and the limited amount of flame data make the knowledge of the H_2O Raman linewidths over the entire temperature range incomplete. Nevertheless it is apparent that very good fits to the flame data have been achieved. The CARS spectrum (Ref. 52) and the concentration that would be inferred from the CARS spectrum is not sensitive to Raman linewidth for $\Gamma >$ 0.2 cm^{-1} at flame temperatures. It is reasonable to assert that, even with limited knowledge of the high temperature linewidths, accurate H_2O thermometry and concentrations measurements can be performed in flames using the computer model described in this contract.

CONCLUSIONS AND RECOMMENDATIONS

Calculations of CARS spectra of H_2O agree very well with experimental spectra over a broad temperature range: 450 to 2100 K at atmospheric pressure. The magnitude and frequency of all features of the experimental spectra are described by the UTRC energy level data set over this temperature range for a spectral resolution ~ 1.5 cm^{-1} or less. The measurements have shown that the spectrum in the bandhead region depends strongly on the H_2O concentration at low to moderate temperature. Computer code calculations indicate that these changes arise from the strong dependence of the Raman linewidth on H_2O concentration. Linewidths have been inferred from the comparison of CARS measurements in the heated cell with calculations and broadening parameters for H_2O, N_2 and CO_2 have been determined. The self broadening coefficient is approximately 2.5 times the coefficient for N_2 and CO_2 broadening, which are comparable. The pure H_2O linewidth decreases with temperature as T^{-1} for low temperature, but the dependence becomes less pronounced at higher temperature, and the linewidth approaches a constant value. These results are in general accord with microwave measurements of the widths of pure rotational transitions.

Based on these observations, it is concluded that the CARS spectrum of H_2O is well understood and can be adequately calculated over a broad temperature range of relevance to combustion. It appears that the concentration of H_2O can be determined from spectral shapes for premixed, hydrocarbon flames. In these flames, the concentration does not rise above the 20 percent level below which there is sufficient modulation for shape measurements. In addition, the background susceptibility and Raman linewidth do not vary much in the post-flame gases of these flames so that the knowledge of these quantities is probably sufficient. For hydrocarbon-fueled diffusion flames, it may be necessary to measure the concentration of other component species before the nonresonant susceptibility can be accurately determined, particularly in regions where the fuel is mixed with H_2O. In hydrocarbon-air flames, the linewidths and nonresonant susceptibility are not expected to be very sensitive to composition, however the H_2O concentration can be as high as 33 percent for a stoichiometric, premixed flame. In this case, the H_2O concentration must be determined from absolute intensities. The linewidth is probably known well enough to permit this, though. For H_2-air diffusion flames, the H_2O concentration probably does not rise above levels where it can be measured from CARS shapes.

Additional measurements of H_2O Raman linewidth broadening coefficients may be helpful. However, the H_2O Raman Q-branch is so dense that it would be impossible to measure the linewidths of individual transitions using CARS with the usual Nd:YAG lasers, because the laser linewidth is broader than the average spacing between lines. It should be possible to operate a well-controlled, single-mode cw oscillator with pulsed amplifiers to make these measurements

with CARS, though. High resolution stimulated Raman gain could also be employed to measure linewidths. Otherwise linewidths must be inferred as was done in this study.

Finally, it should be emphasized that the calculations and experiments of this investigation are for pressures near atmospheric. The theory is not strictly valid when the density is high enough that line overlap causes collisional narrowing effects to become important.

REFERENCES

1. B. Attal, M. Pealat and J. P. E. Taran: CARS Diagnostics of Combustion. AIAA Paper No. 80-0282, 1980.

2. G. L. Switzer, W. M. Roquemore, R. P. Bradley, P. W. Schreiber and W. B. Roh: CARS Measurements in a Bluff-Body Stabilized Diffusion Flame. Appl. Opt., Vol. 18, pp. 2343-2345, 1979. Also AIAA Paper No. 80-0353.

3. A. C. Eckbreth: CARS Thermometry in Practical Combustors. Combust. Flame, Vol. 39, pp. 133-147, 1980.

4. I. A. Stenhouse, D. R. Williams, J. B. Cole and M. D. Swords: CARS in an Internal Combustion Engine. Appl. Opt., Vol. 18, pp. 3819-3825, 1979.

5. D. Klick, K. A. Marko and L. Rimai: Broadband Single-Pulse CARS in a Fired Internal Combustion Engine. Appl. Opt., Vol. 20, pp. 1178-1181, 1981.

6. C. M. Penney and M. Lapp: Scattering Cross Section for Water Vapor. J. Opt. Soc. Am., Vol. 66, pp. 422-425, 1976.

7. J. L. Bribes, R. Gaufres, M. Monan, M. Lapp and C. M. Penney: Raman Band Contours for Water Vapor as a Function of Temperature. Appl. Phys. Letters, Vol. 28, pp. 336-337, 1976.

8. M. Lapp: Raman Scattering from Water Vapor in Flames. AIAA Journal, Vol. 15, pp. 1665-1666, 1977.

9. J. L. Bribes, R. Gaufres, M. Monan, M. Lapp and C. M. Penney: Detailed Study of the Q-Branch Profile of the ν_1 of Water Molecule from 293°K to 1500°K. Proc. 5th Intl. Conf. on Raman Spectroscopy, edited by E. D. Schmid et al., Universitat Freiburg, Sept. 2-8, 1976, Hans Ferdinand Schulz Verlag, Freiburg in Breisgau, 1976.

10. G. E. Walrafen: Raman Spectral Studies of the Effects of Temperature on Water Structure. J. Chem. Phys., Vol. 47, pp. 114-126, 1967, and references contained therein.

11. I. Itzkan and D. A. Leonard: Observations of Coherent Anti-Stokes Raman Scattering from Liquid Water. Appl. Phys. Letters, Vol. 26, pp. 106-108, 1975.

12. R. J. Hall, J. A. Shirley and A. C. Eckbreth: Coherent Anti-Stokes Raman Spectroscopy: Spectra of Water Vapor in Flames. Optics Letters, Vol. 4, pp. 87-89, 1979.

13. W. B. Roh and G. L. Switzer: Application of Coherent Anti-Stokes Raman Scattering to Laser and Combustion Media. R&D Status Report 6948-6, Systems Research Laboratories, Inc., 1978.

14. R. L. Farrow, R. E. Mitchell, L. A. Rahn and P. L. Mattern: Crossed-Beam Background-Free CARS Measurements in Methane Diffusion Flame. AIAA Paper No. 81-0182, 1981.

15. J. W. Nibler, W. M. Shaub, J. R. McDonald and A. B. Harvey: Coherent Anti-Stokes Raman Spectroscopy. In Vol. 6, Vibrational Spectra and Structure, J. R. Durig, Ed. Elsevier, Amsterdam, 1977.

16. A. C. Eckbreth, P. A. Bonczyk and J. F. Verdieck: Combustion Diagnostics by Laser Raman and Flourescence Techniques. Prog. Energy Combust. Sci., Vol. 5, pp. 253-322, 1979.

17. S. Druet and J. P. E. Taran: Coherent Anti-Stokes Raman Spectroscopy. In Chemical and Biological Application of Lasers, C. B. Moore, Ed., Academic Press, New York, 1979.

18. J. W. Nibler and G. V. Knighten: Coherent Anti-Stokes Raman Spectroscopy. In Vol. III, Topics in Current Physics, A. Weber, Ed., Springer-Verlag, Heidelberg, 1979.

19. W. B. Roh, P. W. Schreiber and J. P. E. Taran: Single-Pulse Coherent Anti-Stokes Raman Scattering. Appl. Phys. Letters, Vol. 29, pp. 174-176, 1976.

20. A. C. Eckbreth: BOXCARS: Crossed-Beam Phase-Matched CARS Generation in Gases. Appl. Phys. Letters, Vol. 32, pp. 421-423, 1978.

21. G. Laufer and R. B. Miles: Angularly Resolved Coherent Raman Spectroscopy (ARCS). Opt. Commun., Vol. 28, pp. 250-254, 1979.

22. J. A. Shirley, R. J. Hall and A. C. Eckbreth: Folded BOXCARS for Rotational Raman Studies. Opt. Letters, Vol. 5, pp. 380-382, 1980.

23. Y. Prior: Three-Dimensional Phase Matching in Four-Wave Mixing. Appl. Opt., Vol. 19, pp. 1741-1743, 1980.

24. J. J. Song, G. L. Eesley and M. D. Levenson: Background Suppression in Coherent Raman Spectroscopy. Appl. Phys. Letters, Vol. 29, pp. 567-569, 1976.

25. S. A. Akhmanov, A. F. Bunkin, S. G. Ivanov and N. I. Koroteev: Polarization Active Raman Spectroscopy and Coherent Raman Ellipsometry. Sov. Phys. JETP, Vol. 47, pp. 667-678, 1978.

26. A. F. Bunkin, S. G. Ivanov and N. I. Koroteev: Gas Analysis by Coherent Active Raman Spectroscopy with Polarization Discrimination. Sov. Tech. Phys. Letters, Vol. 3, pp. 182-184, 1977.

27. L. A. Rahn, L. J. Zych and P. L. Mattern: Background-Free CARS Studies of Carbon Monoxide in a Flame. Opt. Commun., Vol. 39, pp. 249-253, 1979.

28. J. L. Oudar, R. W. Smith and Y. R. Shen: Polarization-Sensitive Coherent Anti-Stokes Raman Spectroscopy. Appl. Phys. Letters, Vol. 34, pp. 758-760, 1979.

29. F. M. Kamga and M. G. Sceats: Pulse-Sequenced Coherent Anti-Stokes Raman Scattering Spectroscopy: A Method for Suppression of the Nonresonant Background. Opt. Letters, Vol. 5, pp. 126-128, 1980.

30. A. C. Eckbreth and R. J. Hall: CARS Concentration Sensitivity with and without Nonresonant Background Suppression. UTRC Report R80-954628-1. Prepared for the Office of Naval Research, 1980. --See also: Eckbreth, A. C. and R. J. Hall: CARS Concentration Sensitivity with and without Nonresonant Background Suppression, Comb. Sci. and Tech., Vol. 25, p. 175, 1981.

31. A. C. Eckbreth, R. J. Hall and J. A. Shirley: Inestigations of Coherent Anti-Stokes Raman Spectroscopy (CARS) for Combustion Diagnostics. AIAA Paper No. 79-0083, 1979.

32. J. A. Shirley, R. J. Hall, J. F. Verdieck and A. C. Eckbreth: New Directions in CARS Diagnostics for Combustion. AIAA Paper No. 80-1542, 1980.

33. J. L. Oudar and Y. R. Shen: Nonlinear Spectroscopy by Multi-resonant Four-Wave Mixing. Phys. Rev., Vol. A22, pp. 1141-1158, 1980.

34. G. Herzberg: Molecular Spectra and Molecular Structure II. Infrared and Raman Spectra of Polyatomic Molecules, Van Hostrand, Princeton, N.J., 1945.

35. J. -M. Flaud, C. Camy-Peyret and J. P. Maillard: Higher Ro-vibrational Levels of H_2O Deduced from High Resolution Oxygen-Hydrogen Flame Spectra between 2800-6200 cm^{-1}. Mol. Phys., Vol. 32, pp. 499-521, 1976.

36. C. Camy-Peyret and J.-M. Flaud: Line Positions and Intensities in the ν_2 Band of $H_2{}^{16}O$. Mol. Phys., Vol. 32, pp. 523-537, 1976.

37. C. Camy-Peyret, J.-M. Flaud and R. A. Toth: Vibration-Rotation Intensities for the $3\nu_2$, $\nu_1 + \nu_2$, and $\nu_2 + \nu_3$ Bands of Water (Oxygen-16). J. Mol. Spectrosc., Vol. 67, pp. 117-131, 1977.

38. R. L. St. Peters: Gas Diagnostics Measurement by Coherent Anti-Stokes Raman Spectroscopy: Feasibility Calculations for Water Vapor in Combustion Systems. Final Report under Air Force Systems Command Contract F33615-77-C-311, 1980.

39. A. Weber: High Resolution Raman Studies of Gases, Chap. 8 in The Raman Effect, A. Anderson, Ed., Marcel Dekker, New York, 1973.

40. W. S. Benedict and L. D. Kaplan: Calculation of Line Widths in H_2O-N_2 Collisions. J. Chem. Phys., Vol. 30, pp. 388-399, 1959.

41. W. S. Benedict and L. D. Kaplan: Calculation of Line Widths in H_2O-H_2O Collisions. J. Quant. Spectros. Radiat. Transfer, Vol. 4, pp. 453-469, 1964.

42. P. W. Anderson: Pressure Broadening in the Microwave and Infra-Red Regions. Phys. Rev., Vol. 76, pp. 647-661, 1949.

43. R. G. Gordon: Theory of the Width and Shift of Molecular Spectral Lines in Gases. J. Chem. Phys., Vol. 44, pp. 3083-3089, 1966.

44. R. P. Srivastava and H. R. Zaidi: The Role of Short Range Interaction in Molecular Collision Broadening. Can. J. Phys., Vol. 55, pp. 533-541, 1977.

45. J. L. Bonamy, L. Bonamy and D. Robert: Overlapping Effects and Motional Narrowing in Molecular Band Shapes: Application to the Q Branch of HD. J. Chem. Phys., Vol. 67, pp. 4441-4453, 1977.

46. W. G. Rado: The Nonlinear Third Order Dielectric Susceptibility Coefficients of Gases and Optical Third Harmonic Generation. Appl. Phys. Letters, Vol. 11, pp. 123-125, 1967.

47. F. DeMartini, F. Simoni and E. Santamato: High Resolution Nonlinear Spectroscopy. Dicke Narrowing and Dispersion of the Third-Order Nonlinear Susceptibility of H_2 near the $Q_{01}(1)$ Vibrational Resonance. Opt. Commun., Vol. 9, pp. 176-181, 1973.

48. J. A. Shirley, A. C. Eckbreth and R. J. Hall: Investigation of the Feasibility of CARS Measurements in Scramjet Combustion. NASA Contractor Report 159280, 1980.

49. J. F. Ward and C. K. Miller: Measurements of Nonlinear Optical Polarizabilities for Twelve Small Molecules. Phys. Rev. A, Vol. 19, pp. 826-833, 1979.

50. M. A. Yuratich: Effects of Laser Linewidths on Coherent Anti-Stokes Raman Spectroscopy. Mol. Phys., Vol. 38, pp. 625-655, 1979.

51. R. J. Hall: CARS Spectra of Combustion Gases. Comb. and Flame, Vol. 35, pp. 47-60, 1979.

52. J. A. Shirley, R. J. Hall and A. C. Eckbreth : Investigation of the CARS Spectrum of Water Vapor. Proceedings of the *Lasers '80 International Conference*, 1981. To be published.